AD-778 493

# SPECIAL EVENT DETECTION FOR AN UNATTENDED SEISMIC OBSERVATORY

John S. Eterno, et al

Charles Starr Draper Laboratory, Incorporated

Prepared for:

Air Force Office of Scientific Research

March 1974

DISTRIBUTED BY:

NTIS

National Technical Information Service
U. S. DEPARTMENT OF COMMERCE
5285 Port Royal Road, Springfield Va. 22151

SECURITY CLASSIFICATION OF THIS PAGE (When Data Entered)

## REPORT DOCUMENTATION PAGE

READ INSTRUCTIONS BEFORE COMPLETING FORM

1. REPORT NUMBER: AFOSR - TR - 74 - 0585
2. GOVT ACCESSION NO.
3. RECIPIENT'S CATALOG NUMBER: AD-778 493

4. TITLE (and Subtitle): SPECIAL EVENT DETECTION FOR AN UNATTENDED SEISMIC OBSERVATORY

5. TYPE OF REPORT & PERIOD COVERED: Final Technical, 15 March 73-14 Nov 73

6. PERFORMING ORG. REPORT NUMBER: R-765

7. AUTHOR(s): John S. Eterno, David S. Burns, Lawrence J. Freier, Sheldon W. Buck

8. CONTRACT OR GRANT NUMBER(s): F44620-73-C-0057

9. PERFORMING ORGANIZATION NAME AND ADDRESS: The Charles Stark Draper Laboratory, Inc. Cambridge, Massachusetts 02139

10. PROGRAM ELEMENT, PROJECT, TASK AREA & WORK UNIT NUMBERS: AO 2441

11. CONTROLLING OFFICE NAME AND ADDRESS: Advanced Research Propects Agency/NMR, 1400 Wilson Boulevard, Arlington, Virginia 22209

12. REPORT DATE: March 1974

13. NUMBER OF PAGES: 79

14. MONITORING AGENCY NAME & ADDRESS (if different from Controlling Office): Air Force Office of Scientific Research/NP, 1400 Wilson Boulevard, Arlington, Virginia 22209

15. SECURITY CLASS. (of this report): UNCLASSIFIED

15a. DECLASSIFICATION/DOWNGRADING SCHEDULE

16. DISTRIBUTION STATEMENT (of this Report)

Approved for public release; distribution unlimited.

17. DISTRIBUTION STATEMENT (of the abstract entered in Block 20, if different from Report)

DDC RECEIVED MAY 30 1974 REGISTERED F

18. SUPPLEMENTARY NOTES

Reproduced by NATIONAL TECHNICAL INFORMATION SERVICE U S Department of Commerce Springfield VA 22151

19. KEY WORDS (Continue on reverse side if necessary and identify by block number)

Seismic detection
Event detection
Nuclear explosion detection
Unattended seismic observatory
Data acquisition

20. ABSTRACT (Continue on reverse side if necessary and identify by block number)

A practical event detection system for monitoring remote three-axis seismometers is described. The self-contained system, through use of digital storage, records data from 30 seconds before an event is triggered until earth motion subsides. Intended for use in an unmanned seismic observatory, the device is capable of detecting near events as well as the multiple phases of teleseisms. Provision has been made for the on-site adjustment

DD FORM 1 JAN 73 1473 EDITION OF 1 NOV 65 IS OBSOLETE



SECURITY CLASSIFICATION OF THIS PAGE (When Data Entered)

20. ABSTRACT (continued)

of critical detection parameters. A prototype has been tested on prerecorded data at the Vela Seismological Center in Alexandria, Virginia. A summary and interpretation of the test results is included.

R-765

# SPECIAL EVENT DETECTION FOR AN UNATTENDED SEISMIC OBSERVATORY

by

John S. Eterno
David S. Burns
Lawrence J. Freier
Sheldon W. Buck

March 1974

Approved: _____
Philip N. Bowditch

ARPA Order No. – 2441
Project Code No. – 3F10
Name of Contractor – The Charles Stark Draper Laboratory, Inc.
Date of Contract – March 15, 1973
Contract Expiration Date – November 14, 1973
Amount of Contract – $59,000
Contract No. – F44620-73-C-0057
Principal Investigator – Sheldon W. Buck (617) 258-1531
Project Engineer – Lawrence J. Freier (617) 258-4009
Short Title of Work – "Unattended Seismic Observatory Event Detector"

Approved for public release; distribution unlimited.

ii

## ACKNOWLEDGMENT

This research was supported by the Advanced Research Projects Agency of the Department of Defense and was monitored by the Air Force Office of Scientific Research under Contract No. F44620-73-C-0057.

The authors wish to express their appreciation to the following personnel for their contributions to our work:

Captain John Bailey, USAF, for arranging our use of the analog computer facility at the Vela Seismological Center in Alexandria, Va.

Messrs. John Woolfson and Charles Cowden of Teledyne, Inc., Alexandria, Va., for their assistance during our testing at Vela.

Messrs. Richard T. Lacoss and Robert M. Sheppard, Jr. of the Lincoln Laboratory at MIT for their aid in the design and preliminary testing of our event detection methods.

Publication of this report does not constitute approval by the U.S. Air Force of the findings or conclusions contained herein. It is published for the exchange and stimulation of ideas.

TABLE OF CONTENTS


| Section | | | Page |
|---|---|---|---|
| 1 | INTRODUCTION. . . . . | | 1 |
| 2 | USO SYSTEM OVERVIEW . . . . . | | 3 |
| 3 | EVENT DETECTION . . . . . | | 9 |
| | 3.1 Theory . . . . . | | 9 |
| | | 3.1.1 Detection of a Known Signal in White Noise. | 9 |
| | | 3.1.2 Detection of an Unknown Signal in White Noise . . . . . | 10 |
| | | 3.1.3 Practical Constraints . . . . . | 11 |
| | | 3.1.4 Band-Pass Filtering . . . . . | 12 |
| | 3.2 Detector Design Verification . . . . . | | 13 |
| | | 3.2.1 Data Tape . . . . . | 13 |
| | | 3.2.2 Detector Simulation . . . . . | 14 |
| | | 3.2.3 Simulation Results. . . . . | 14 |
| | 3.3 Event Duration Control . . . . . | | 16 |
| | | 3.3.1 Delay Line for Pre-Event Recording. . . . . | 16 |
| | | 3.3.2 "End-of-Event" Detection. . . . . | 16 |
| | 3.4 First Vela Test Series . . . . . | | 16 |
| | | 3.4.1 Description of Test . . . . . | 16 |
| | | 3.4.2 Test Conclusions. . . . . | 20 |
| 4 | DETAILED CIRCUIT DESIGN . . . . . | | 23 |
| | 4.1 Anti-Aliasing Filters. . . . . | | 23 |
| | 4.2 A/D conversion . . . . . | | 24 |
| | 4.3 Event Detector . . . . . | | 25 |
| | 4.4 30-Second Buffer Memory. . . . . | | 26 |
| | 4.5 Station Timekeeping. . . . . | | 28 |
| | 4.6 Tape Recorder. . . . . | | 28 |
| | 4.7 Power Budget . . . . . | | 30 |
| | 4.8 Summary. . . . . | | 30 |

TABLE OF CONTENTS (continued)


| Section | | Page |
|---|---|---|
| 5 | SECOND SERIES OF TESTS AT VELA. . . . . | 35 |
| | 5.1 System Modifications . . . . . | 35 |
| | 5.2 Test Results . . . . . | 36 |
| | 5.2.1 Band-Pass Filters . . . . . | 36 |
| | 5.2.2 Energy Averages . . . . . | 37 |
| | 5.2.3 Threshold Levels. . . . . | 37 |
| | 5.2.4 Digital Smoothing . . . . . | 38 |
| | 5.2.5 Event Duration. . . . . | 39 |
| | 5.2.6 Simultaneous Three-Axis Operation . . . . . | 41 |
| | 5.3 Discussion of Results. . . . . | 42 |
| 6 | CONCLUSION. . . . . | 45 |

| Appendix | | |
|---|---|---|
| A | EVENT DETECTOR SCHEMATIC. . . . . | A-1 |
| B | BAND-PASS FILTER FREQUENCY RESPONSES. . . . . | B-1 |
| C | 30-SECOND MEMORY QUOTE COMPARISON . . . . . | C-1 |
| D | DATA FROM VELA TESTS. . . . . | D-1 |
| | LIST OF REFERENCES . . . . . | R-1 |

LIST OF ILLUSTRATIONS


| Figure | | Page |
|---|---|---|
| 2-1 | Block diagram for USO system. | 5 |
| 3-1 | Operation of ideal receiver | 10 |
| 3-2 | Operation of a practical event detector | 12 |
| 3-3 | Computer simulation of event detector operation | 15 |
| 3-4 | Initial event detector design | 17 |
| 3-5 | Event detector breadboard | 18 |
| 3-6 | Modified shut-off logic | 19 |
| 4-1 | Simulated event detector operation. | 27 |
| 5-1 | Event detector recording time (without 30-second pre-event memory) for parameters listed in Table 5-2. | 40 |
| A-1 | Single-channel event detector | A-5 |
| B-1 | Vertical-channel band-pass filter options | B-3 |
| B-2 | Horizontal-channel band-pass filter options | B-4 |
| D-1 | "Cashmere" recorded at RKON | D-5 |
| D-2 | "Cashmere" recorded at TFO. | D-7 |
| D-3 | "Merlin" recorded at RKON | D-9 |
| D-4 | "Merlin" recorded at TFO. | D-11 |
| D-5 | Uncatalogued event recorded at TFO. | D-13 |

LIST OF TABLES


| Table | | Page |
|---|---|---|
| 3-1 | Events on test tape. . . . . | 14 |
| 3-2 | First Vela test summary. . . . . | 21 |
| 4-1 | 30-second memory component comparison. . . . . | 29 |
| 4-2 | Event detector power budget. . . . . | 31 |
| 4-3 | Performance characteristics of the event detector. . . . . | 32 |
| 5-1 | Total number of false triggers and events on both horizontal event-detector channels during an 8-minute tape section. . . . . | 39 |
| 5-2 | Effects of parameter changes on the recording command. . . | 41 |
| A-1 | Center frequency of band-pass filter . . . . . | A-3 |
| A-2 | Time constant of the long-term averager. . . . . | A-3 |
| A-3 | "Signal/noise" threshold level . . . . . | A-4 |
| A-4 | Channel-dependent values . . . . . | A-4 |

# SECTION 1

# INTRODUCTION

This report presents our design of an event detection system for an Unattended Seismic Observatory (USO). Event detectors, in general, can reduce magnetic tape usage, data transmission requirements, and data analysis time at a central receiving station. These advantages are obtained by screening the incoming data for seismic events "worth recording". Our application of these techniques to an unattended, remote observatory using borehole seismometers stresses low power, high-reliability circuitry, and small package size for "down-hole" installation. The design provides for the remote adjustment of critical detection parameters in order to tune the detector to a particular site location.

An interesting feature of our system is the use of an independent detector on each of the three short-period channels (vertical, north, and east). This feature was originally incorporated (a single vertical detector being more common) to provide a better probability of detecting a nearby event (this being a primary goal of the USO program). We felt that the shear wave energy near the source would be high enough to provide a reliable trigger. In fact, the three-axis system finally developed was not only able to detect nearby events on all three channels (providing our desired backup) but could also detect the separate phases of teleseisms. In particular, the horizontal detectors could locate delayed S-waves that the vertical channel missed.

This report is organized in the following manner. Section 2 describes the goals of the USO program and outlines a system that we have developed to implement these objectives. This description gives an overview of our task and provides a framework in which to view our detector design. Section 3 summarizes the relevant theory of event detection and applies this theory to our design problem. It also describes a preliminary design, summarizes test results, and explains the resulting modifications. Section 4 gives a detailed analysis of the major components

of our system. This investigation includes, among other topics, the signal-conditioning filters, analog-to-digital conversion requirements, and the event detector circuit design. Section 5 analyzes the results of advanced tests made with a prototype of our event detector design. These tests demonstrated the good performance of the design and motivated future improvements. Section 6 summarizes the results of our work and suggests future areas of research.

In conclusion, we would like to mention the generality of our results. The event detector, while developed expressly for USO use, does not contain any features that restrict its use to that application. On the contrary, the primary results of our designing from the start for a remote installation would be beneficial to any seismic station. Low power, small size, high reliability, and the on-site adjustment of critical parameters would be useful in any foreseeable detector application.

## SECTION 2

## USO SYSTEM OVERVIEW

The Unattended Seismic Observatory (USO) was intended to be a self-contained automatic system for the acquisition, recording, and transmission of seismic data. Earth motion would be sensed along three orthogonal axes (vertical, north, and east), in each of two frequency bands: long period (< 0.1 Hz), and short period (> 0.2 Hz). We assumed that the seismometers would have similar response curves to those specified in the Seismic Research Observatory (SRO) "request for proposals", shown in Figure 2-1 (on the far left). These responses may be obtained from separate long- and short-period instruments, or they may be separate long- and short-period filters acting on broad-band sensors.

The seismometers would be mounted approximately 1000 feet underground in a 7-inch (nominal) diameter borehole. The seismometer outputs would be digitized and recorded on a single magnetic tape in a format permitting easy data recovery and time decoding. The entire USO system would be sealed with an anti-intrusion system, and the data passed through an authenticator circuit. Data retrieval would be accomplished through periodic tape pickup or, perhaps, through satellite transmission to a central receiving station.

The system would operate in the following manner (see Figure 2-1). Each long-period channel would be sampled once per second. This provides an adequate representation of the signal at a low enough data rate to allow continuous recording of the three long-period channels. The short-period channels, however, require a higher sampling rate to capture their higher frequency information. A 20-Hz sample rate appears to be a suitable compromise between signal fidelity and tape usage. This rate, however, still uses 20 times as much tape as the long-period channels. While we intended to record long-period data continuously, we felt that some method of screening the short-period data for interesting information was justified.

We therefore planned to incorporate an event detector into our design for the short-period channels. This circuit would be able to screen the incoming short-period data, detect the events of interest (earthquakes and underground nuclear explosions), and signal the recorders. This would allow us to save considerable magnetic tape, "compress" the data for transmission, and reduce later processing at a central receiving station monitoring a number of remote USOs.

We wanted to use analog event detector circuitry for reasons of simplicity and reliability. Since we intended to record our data digitally after transmitting it up from the borehole, placing the analog-to-digital (A/D) converter down-hole with the seismometers made sense. This arrangement implied that the event detector be mounted down-hole operating on the analog data before conversion.

Since any event detector would take a finite amount of time to respond, the actual detector signal to start recording would occur after the beginning of an event. The "first motion" is important in analyzing the data, as is the pre-event noise level. Rather than miss these signals entirely, we planned to save 30 seconds of past data while the event detector reacted. All the short-period data would be digitized and routed through a shift-register "delay line". When an event was declared, the recorder would be turned on, catching the end of the shift-register data. When no event was sensed, the register would be allowed to overflow (dumping the background noise data).

All of the data worth recording (long-period signals and short-period events) would be formatted in accordance with an anti-intrusion and authentication circuit developed by Sandia Corporation. If such a device is incorporated, we will essentially input our data to it, and receive a signal to record and transmit from it. It will have power and space requirements also, but these are considered outside of the scope of this report. We will, therefore, describe our system without reference to the authenticator; it may be incorporated or omitted at will.*

The final data form may be transmitted via satellite for use at a central receiving station. At present, the power and cost requirements

---

*The formatting of our data into 1024-bit blocks for input to the authenticator will be described in a subsequent report.

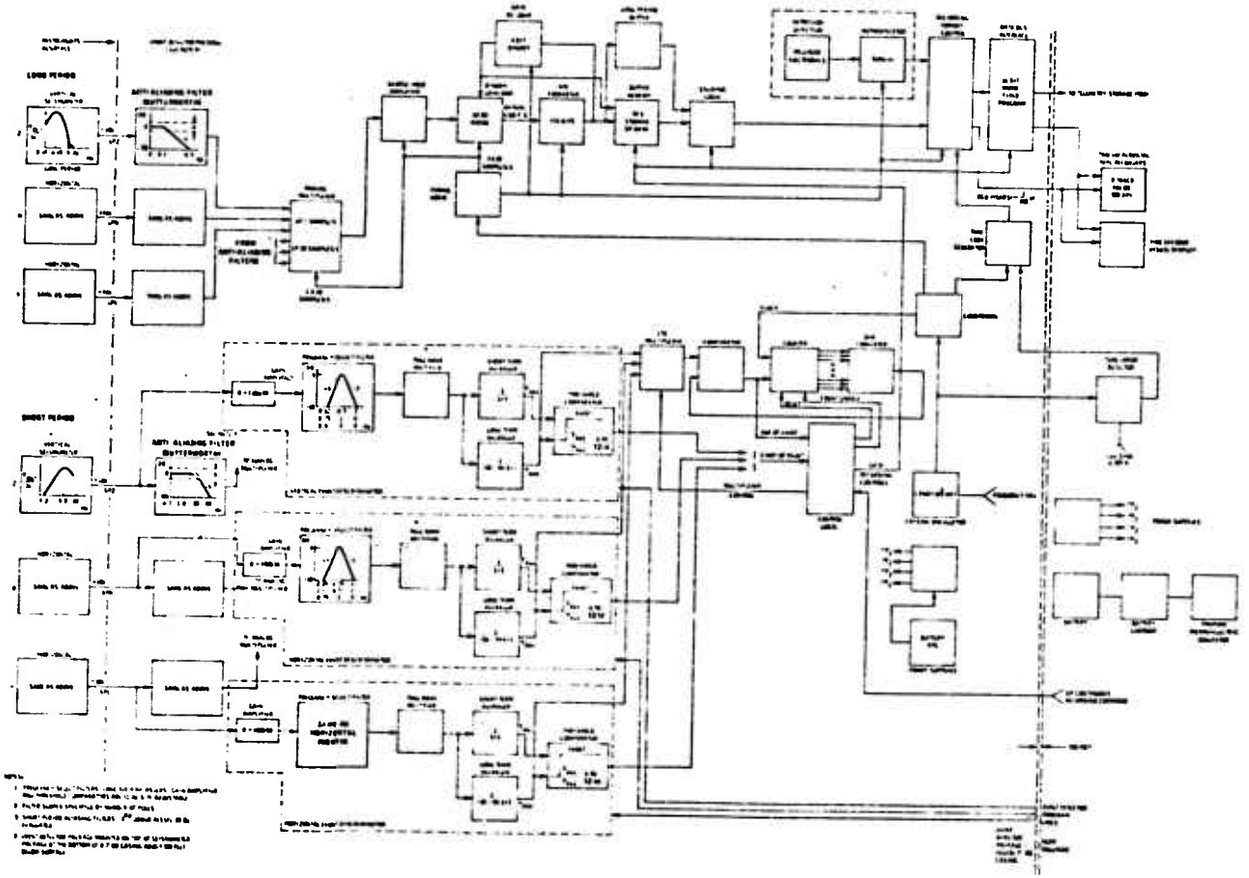
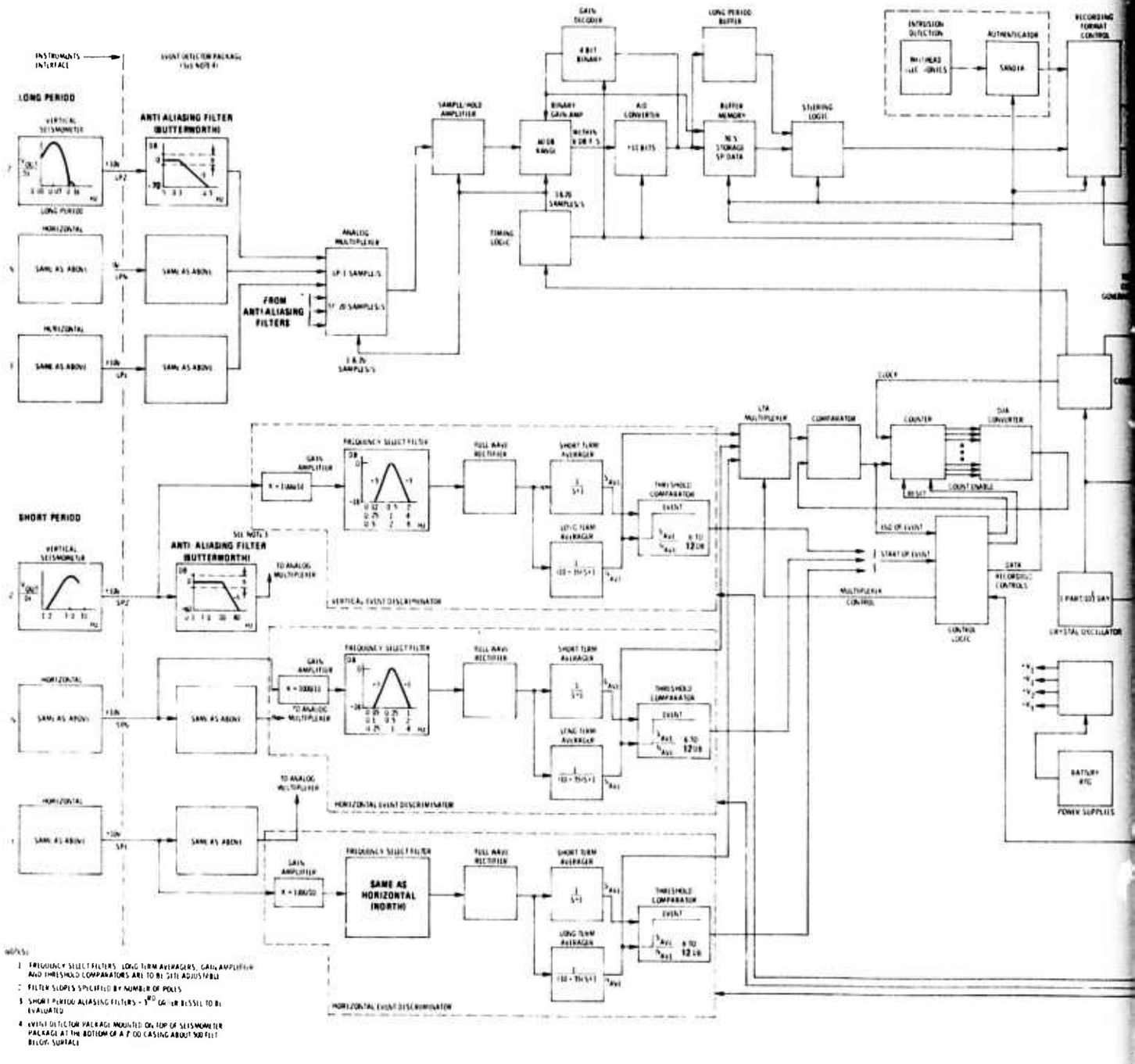


Figure 2-1. Block diagram for USO system.



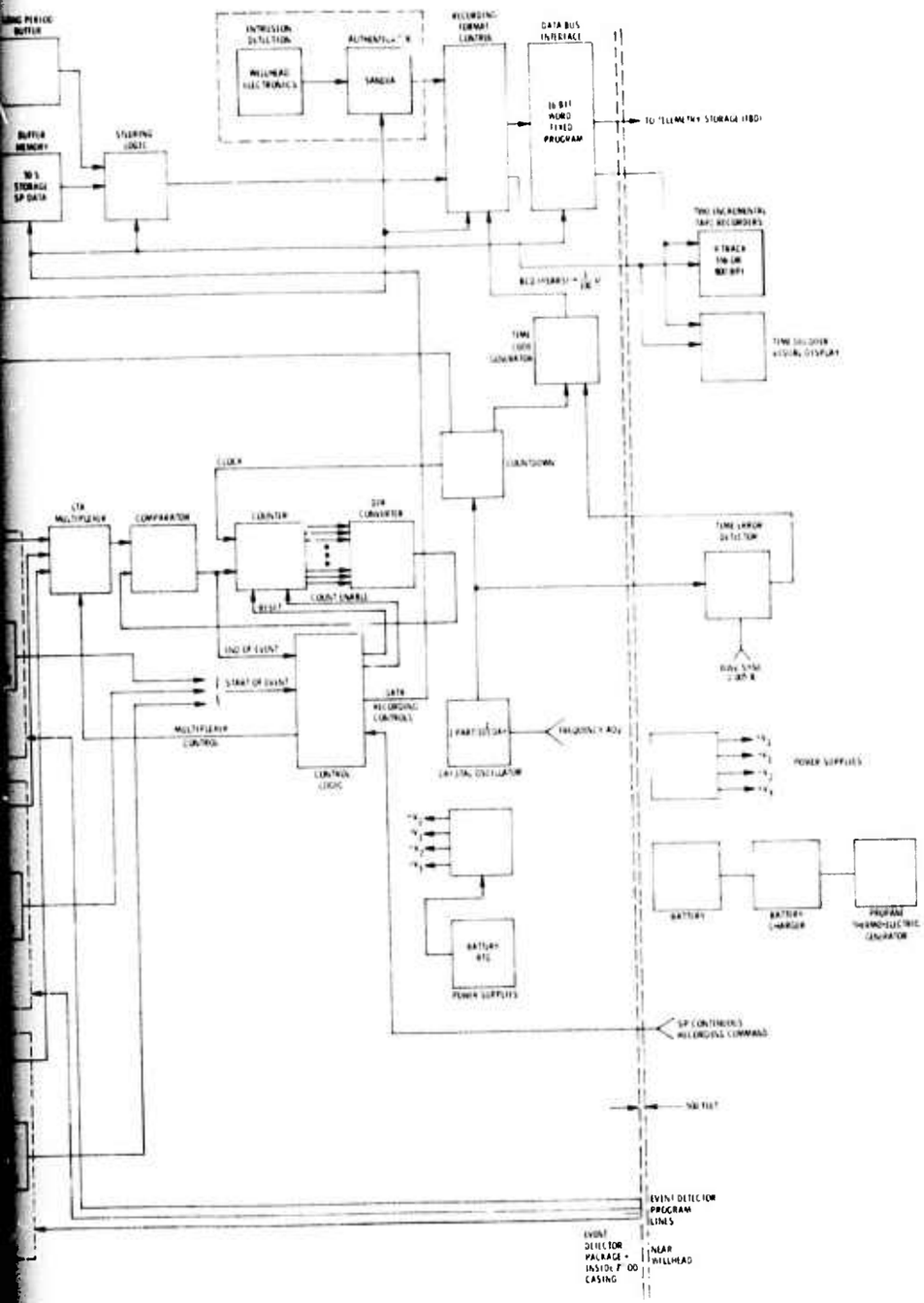
XXXXXXXXXXXXXXXXXXXXXX
See the following pages
for greater detail.
XXXXXXXXXXXXXXXXXXXXXX




NOTES:

1. FREQUENCY SELECT FILTERS, LONG TERM AVERAGERS, GAIN AMPLIFIER AND THRESHOLD COMPARATORS ARE TO BE SITE ADJUSTABLE
2. FILTER SLOPES SPECIFIED BY NUMBER OF POLES
3. SHORT PERIOD ALIASING FILTERS - 3RD ORDER BESSEL TO BE EVALUATED
4. EVENT DETECTOR PACKAGE MOUNTED ON TOP OF SEISMOMETER PACKAGE AT THE BOTTOM OF A 7.00 CASING ABOUT 900 FEET BELOW SURFACE

Figure 2-1. Block diagram for USO system.




agram for USO system.

of the transmitter far outweigh those of the rest of the station, and periodic tape pickup may be a better choice for the primary means of data retrieval.

The main thrust of our work has been in the event-detection portion of the unattended seismic observatory. However, the event detector we developed would be useful in any seismic data retrieval system and may be regarded as a self-contained device. The savings in magnetic tape, strip-chart recorder paper, and analysts' time would make it an attractive option even for a manned observatory.



Preceding page blank

SECTION 3

EVENT DETECTION

## 3.1 Theory

A great deal of theory exists for event detection. This section will summarize the relevant theoretical results, design an "optimum" detector for seismic signals, and describe the approximations that we found practical to make in our seismic event detector.

### 3.1.1 Detection of a Known Signal in White Noise

Let us suppose that we are trying to use a received signal $z(t)$ to determine whether or not a known signal $s(t)$ was transmitted over a noisy channel during the time interval $0 \leq t \leq T$. Then there exist two hypotheses ($H_1$ and $H_2$) concerning what might have occurred in the interval:

$$H_1 : z(t) = \sqrt{A}\, s(t) + n(t), \quad \text{for } 0 \leq t \leq T$$

$$H_2 : z(t) = n(t) \quad , \quad \text{for } 0 \leq t \leq T$$

where $s(t)$ is a known signal and $n(t)$ is a zero-mean white Gaussian noise process with a correlation function* of

$$E\{n(t)\, n(\tau)\} = R\, \delta(t-\tau)$$

We let $\int_0^T s^2(t)\, dt = 1$ for convenience, so that A represents the transmitted signal energy, and $n(t)$ can be thought of as measurement (channel) noise.

*where $E\{\ \}$ is the expectation operator and $\delta$ is the Dirac delta function. This is the standard definition of white noise in the time domain. The reader may be more familiar with the equivalent definition of a "flat frequency spectrum" of height R.

Then, because of the whiteness (lack of time correlation) of n(t), we can find a function of the measurement z(t) that incorporates all of the information needed to select a hypothesis. This function, $\ell'$, of z(t) is often called a "sufficient statistic", and for our problem it may be shown to be[1]*

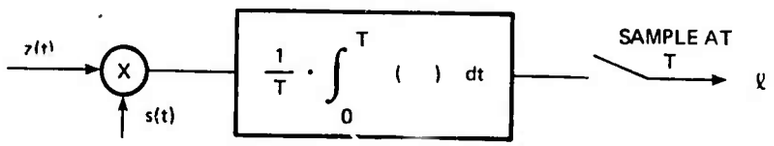
$$\ell' = \int_0^T s(t)\, z(t)\, dt$$

This design is often called a correlation receiver, since it correlates the transmitted signal s(t) with the received signal z(t). Once $\ell'$ is obtained, the decision is made on the basis of

If $\ell' \geq \eta' \sqrt{A}$, choose $H_1$ to be true;

otherwise, choose $H_2$

where $\eta'$ represents an adjustable "threshold", dependent on our evaluation of the costs of making a mistake on our choice of hypotheses. For instance, if our declaring $H_1$ to be true when $H_2$ really occurred (a "false alarm") is very costly to us, we may make $\eta'$ very large so that $H_1$ is seldom chosen. Similarly, if the most risk lies in missing an event, we may make $\eta'$ very small so that $H_1$ is chosen often. For convenience, we multiply both $\ell'$ and $\eta'$ by $\frac{1}{T}$ (forming $\ell$ and $\eta$, respectively) to arrive at an equivalent test, shown in Figure 3-1.




If $\ell > \eta \cdot \sqrt{A}$, choose $H_1$.

Figure 3-1. Operation of ideal receiver.

3.1.2 Detection of an Unknown Signal in White Noise

We may now generalize the results above to the case where s(t) is completely unknown. Intuitively, we should expect similar results if we replace s(t) in the receiver above with our best estimate of s(t). Since s(t) is unknown, a reasonable estimate of s(t) is the received signal z(t). The detector statistic is thus

$$\ell = \frac{1}{T} \cdot \int_0^T [z(t)]^2\, dt$$

* Superscript numerals refer to similarly numbered references in the List of References.

If a signal is present ($H_1$), $\ell$ approximates A + R, where A is the (unknown) signal energy, and R is the energy of the white noise. If no signal is present ($H_2$), $\ell$ approximates R alone. A suitable test would therefore be:

$$\text{If } \ell \geq \eta \, R, \text{ choose } H_1$$

$$\text{otherwise choose } H_2$$

That is, if our statistic $\ell$ is sufficiently greater than the expected noise energy, R, we conclude "something else" (our signal) was present in addition to n(t) during the measurement interval $0 \leq t \leq T$.

### 3.1.3 Practical Constraints

We now attempt to simplify computation of the detector statistic, $\ell$, above. The squaring of z(t) before its integration would require very good (expensive) analog components or excessive digital computation time. IBM, in their investigation of an event detector design,[2] found that they could effectively approximate the squaring function with a full-wave rectifier, i.e.,

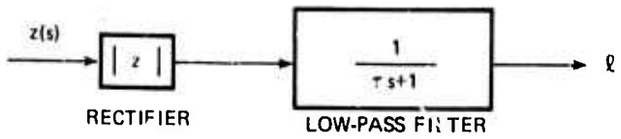
$$[z(t)]^2 \simeq |z(t)|$$

This approximation becomes poorer as the signal-to-noise (energy) ratio increases. For a good event detector, however, operating with signal-to-noise ratios near 1, the approximation was deemed worthwhile.

The time averaging of the rectified signal may also be simplified. Since we are looking for a seismic wave front in real time, we can assume that measurements far in the past are of less value than those immediately before the current time. We may, therefore, exponentially weight the rectified received signal and integrate the weighted value. This would allow a simple low-pass filter to be used in place of the pure integrator. Our sufficient statistic then becomes

$$\ell = \int_0^T e^{-\frac{1}{\tau}(T-t)} \, |z(t)| \, dt$$

And the detector thus looks like Figure 3-2 (in the Laplace domain).




If $\ell > \eta \cdot R$, decide "an event has recently begun".

Figure 3-2. Operation of a practical event detector.

In the case of seismic event detection, the noise energy, R, may vary from day to day. We chose to estimate R dynamically and built this feature into our detector in the following manner. We put the signal z(s) through an operation identical to that above, this time ending with a very low-pass filter (long $\tau$). Thus, we observe a "signal energy" $\ell$, and a "noise energy" in the dc component of $\ell$. If $\ell$ increases by a suitable factor, $\eta$, in a short period of time, we conclude that a seismic event has recently occurred.

For simplicity, and because the $\tau$ for the noise estimate is much longer than the $\tau$ for the signal, we simply stack the noise low-pass filter after the signal low-pass filter. By convention, the signal out of the first low-pass filter, our signal energy estimate, is called the "Short-Term Average" (STA), while the second filter's output, our noise estimate, is known as the "Long-Term Average" (LTA). Our detector criterion is

$$\text{If } \frac{\text{STA}}{\text{LTA}} \geq \eta, \text{ then decide that "an event has recently begun"}$$

### 3.1.4 Band-Pass Filtering

One remaining feature of our event detector which should be discussed is the band-pass filter. It was felt that the raw seismometer output (on a short-period instrument) was not the best possible signal for event detection. A seismic event may start as a pure pressure pulse, quickly generating pressure and shear waves in a wide frequency band. The mantle of the earth, however, acts as a low-pass filter on these waveforms, rapidly attenuating the higher frequencies with distance. Indeed, above 10 Hz almost all recorded signals are due to local "cultural" noise (e.g., trucks).

On the low-frequency end of the short-period seismometer's response is the 0.16-Hz (6-second) microseism region. We are thus led to consider the band between 0.2 and 10 Hz. We have found that the best signal-to-noise ratio for vertical seismometers appears to exist around 1 Hz. A lot of energy from "close-in" events exists above this figure, but even in these cases there appears to be suitable energy in the 1-Hz region to ensure detection. For teleseisms seen on the vertical channel, the 1-Hz region appears optimum. For the horizontal channels, since shear waves suffer a greater attenuation with distance than pressure waves, a frequency slightly lower than 1 Hz might be better.

In light of these ideas, we felt that a band-passed seismometer output would provide a better signal-to-noise ratio than the raw signal for detection. We therefore used band-pass filters with a 1-Hz center frequency (-3 dB points at $\pm 1$ octave) for our vertical channel event detector, and with a 1/2-Hz center frequency (-3 dB points at $\pm 1$ octave also) for the horizontal channels.

The description of our event detector design is now nearly complete. The vertical-channel seismometer output is band-pass filtered, rectified, and passed through two low-pass filters (STA and LTA) for energy computations. When the STA is greater than $\eta \cdot$ LTA, an event is declared.

We also use a nearly identical detector (different center frequency and $\eta$) on each of the two orthogonal horizontal channels. Independent horizontal detectors were regarded as optimum for the detection of events on one axis, while suffering only a 3-dB ($\sqrt{2}$) detection degradation in signal-to-noise ratio for events at 45° angles to the seismometers. Furthermore, we thought that two independent horizontal detectors were less susceptible to failure than a single (composite) unit. Thus, our design incorporates three independent event detectors of identical design, with the provision made for separate parameter adjustment of the center frequencies, thresholds and time constants on each of the units.

## 3.2 Detector Design Verification

### 3.2.1 Data Tape

In an attempt to get a baseline for event detector performance, a composite magnetic tape of five seismic events (explosions and earthquakes) was made from the data library at Lincoln Laboratory for use

with a computer simulation of our design. The 40-minute tape represented a wide range of signal strengths in events from 3 to 12 degrees from the recording seismometer in the LASA array in Montana.[3] The four data channels on the tape included two vertical and two horizontal short-period sensors, with the horizontal units at the same location in the array as the second vertical channel. The events are listed in Table 3-1.

Table 3-1. Events on test tape.

| Event | Type | Location | Δ (degrees) | Magnitude |
|---|---|---|---|---|
| 1 | Earthquake | Montana | 5.6 | 4.2 |
| 2 | Quarry Blast | British Columbia | 6.5 | 4.4* |
| 3 | Quarry Blast | British Columbia | 6.5 | 5.0* |
| 4 | Earthquake | Yellowstone | 3.5 | 4.2 |
| 5 | Nuclear Test | Nevada | 12.0 | 5.3 |

*These magnitudes were derived from only a few local stations; the signals as received were quite small.

### 3.2.2 Detector Simulation

A FORTRAN program was written to filter this tape and compute short- and long-term average energy levels (STA and LTA, respectively), then display their quotient STA/LTA versus time. It was felt that this would provide the most useful information for evaluating different detector designs. The program effectively simulated the event detector design in our proposal, while being general enough to incorporate other designs for comparison.

### 3.2.3 Simulation Results

The preliminary results were encouraging. The vertical-channel "triggers" were sharp and large (see Figure 3-3). The horizontal triggers were not as large for these close-in events, but it was felt that this would improve as we looked at events further away, where the time difference between P- and S-waves is greater, so that the S-wave detector would not be misled by the horizontal component of the P-wave.

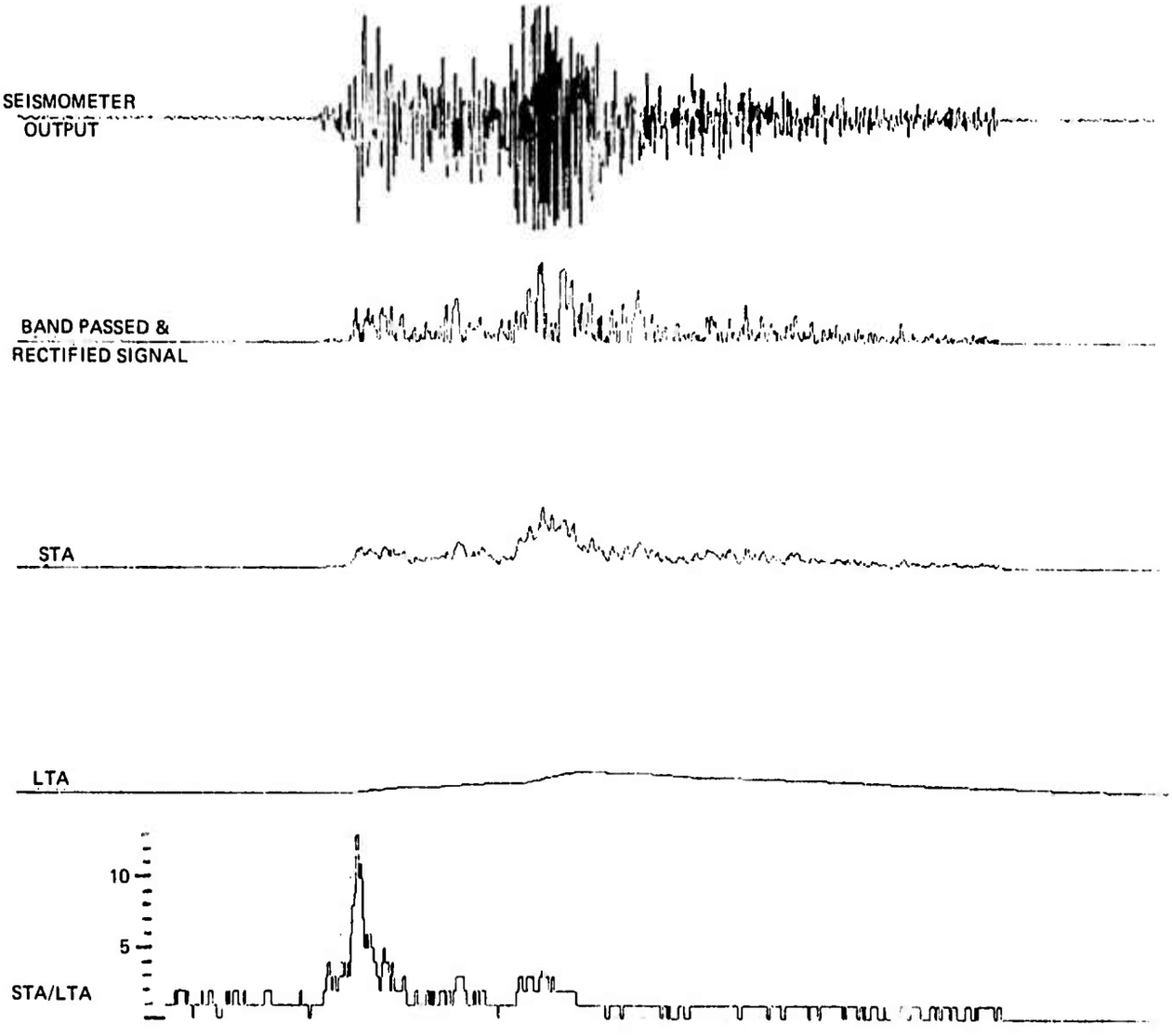



Figure 3-3. Computer simulation of event detector operation.

## 3.3 Event Duration Control

### 3.3.1 Delay Line for Pre-Event Recording

The purpose of our event detector is the detection and recording of seismic events. Considering the importance of the "first motion" received from each signal, and knowing that our detector would not detect the first few seconds of an event (time is needed for the STA to respond), we felt that a certain amount of data immediately preceding event declaration would have to be recorded. This is accomplished through use of a 30-second digital "delay line". All short-period seismic data (after anti-alias filtering) is sampled and converted to a digital format (16-bit data words sampled at a 20-Hz rate per channel). These data words are sent through a shift register capable of holding 30 seconds worth of data. As soon as an event is declared, the output of the shift register is recorded (normally, when no event is sensed, the output is dumped), while "new" information is still pumped through the register 30 seconds "late".

### 3.3.2 "End-of-Event" Detection

The second problem concerning the data recording is the question of when to turn off the recorders: end-of-event detection. An event could be declared "over" when the computed signal-to-noise ratio (STA/LTA) falls below $\eta$. However, during an event of any significant size, the event energy would enter the LTA, causing it to indicate a far higher value than the real background noise level. In an attempt to find a better indication of when an event was over, we decided to "freeze" the LTA when an event was declared. Thus the signal energy would have to fall below – or within $\eta$ of – the pre-event noise level in order to shut off. Our first full event detector (for one channel) is shown in Figure 3-4.

## 3.4 First Vela Test Series

### 3.4.1 Description of Test

This design was incorporated in a breadboard circuit and tested on (analog) recorded events at the Vela Seismological Center in Alexandria, Virginia in early September 1973. We wanted to use recorded events because we wanted a repeatable test input with which to evaluate different

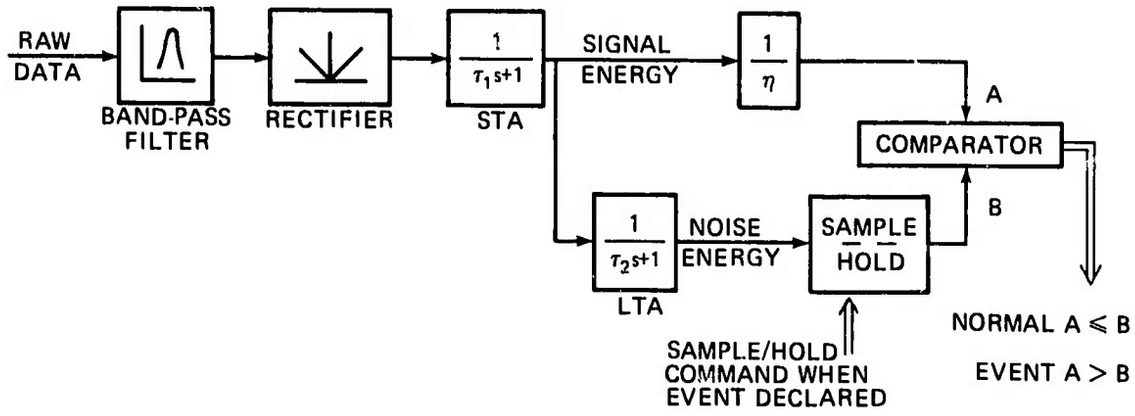



Figure 3-4. Initial event detector design.

settings of our adjustable parameters. The Vela Center has an excellent tape library from which we selected a series of recordings from different stations. We selected recordings of three channels of simultaneous data so that the relative trigger times of the horizontal and vertical detectors could be investigated.

The prototype of our design is shown in Figure 3-5. We played back the recorded signals through Vela equipment and input the three raw data channels to our device. We used a commercial digital voltmeter (also illustrated) for the A/D conversion necessary for freezing the LTA. Our breadboard output was sent to a strip-chart recorder where we recorded the raw data, STA, LTA, and (binary) trigger signal for each channel in addition to the event duration signal and a timing channel. (Examples of our recorded data appear in Appendix D.)

The event duration signal for this prototype only relied on the frozen LTA from the channel which first triggered a particular event. Our proposed system would utilize three event duration signals and continue recording for as long as any one indicated an event was still in progress. This feature is currently under investigation, and may be included in a later prototype if time permits. (See Section 5.2.6 for further discussion.)

The initial test results were not entirely satisfactory. The STA contained more "ripple" during an event than was expected, so that a valley in the STA, hardly representing the end of the event, would cause a premature shutoff. The peak after this valley would often turn the

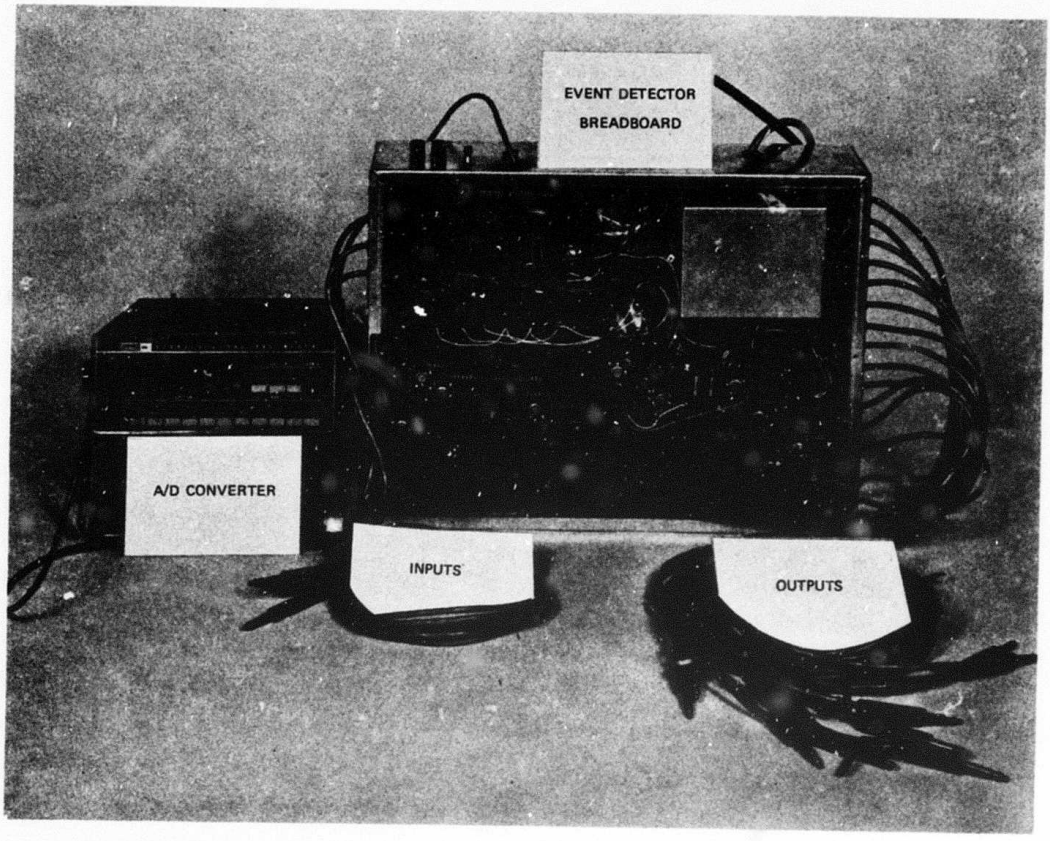



Figure 3-5. Event detector breadboard.

system on again, but by then the LTA had built up during the period since the event started, so that the second turnon froze an artificially high noise estimate.

In order to derive a more reliable turn-off signal, the breadboard was modified at Alexandria to compare the LTA (real) with the frozen LTA for the turn-off criteria. This scheme is shown in Figure 3-6. The turn-on indication was not changed, but once an event was declared, the LTA was sent to the comparator (as "A" in the figure) instead of the STA. Then the system would turn off when the long-term energy approached the pre-event noise level.

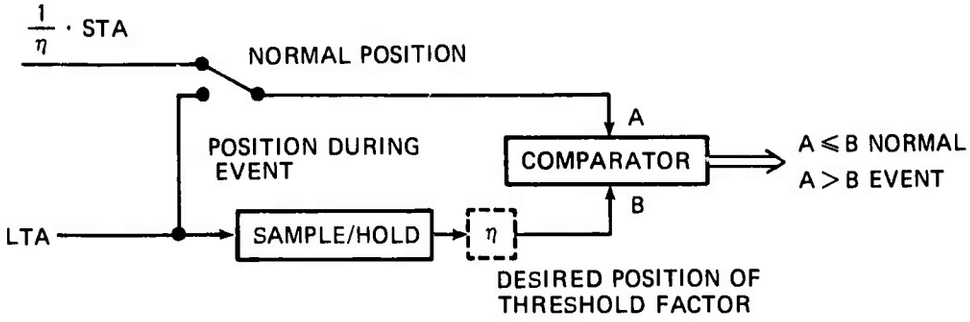



Figure 3-6. Modified shut-off logic.

Unfortunately, in the original system, the threshold was used to attenuate the STA, rather than amplify the LTA, and we could only modify the system to that shown above within the allotted time. We would have liked some attenuation of LTA (real) during an event so that the noise need only approach, not go below, its prior value to turn off the system. This situation was alleviated somewhat in the breadboard due to a 1 to 2-second delay in the sample/hold, so that the LTA increased a little before being frozen (if an event was there). This is not considered ideal (since a false alarm would result in much tape loss waiting for the noise level to decrease), and we are currently investigating alternatives for an operational system (see Section 5.1). Nonetheless, much useful information was gained with the configuration of Figure 3-6.

At first, with $\tau_2$ = 50 seconds (LTA), the system waited too long after the end of an event before shutting off. Our previous tests at Lincoln Laboratory had indicated that $\tau_2$ = 50 seconds provided a good detect criteria, however, and we thought that $\tau_2$ = 10 seconds would be too short, since an "emerging" event (one with a slow buildup) would cause the LTA to rise almost as quickly as the STA. We were able to modify the vertical channel (the most accessible) to include the intermediate values of $\tau_2$ = 17 and $\tau_2$ = 37 seconds, at the expense of the unused very long-term $\tau_2$ = 160 seconds. In our remaining tests at Vela, $\tau_2$ = 17 seconds appeared to give good results for turnon, and yet died down quickly enough after an event to provide a good end-of-event indication. This also meant that the system was "ready" to pick up a second event on the tail of the first (as it did with a Philippine earthquake after a Nevada test).

The final modification to be made at Alexandria was the alteration of the threshold ($\eta$) range. We originally considered the options of $\eta$ = 6, 12, and 18 dB (a factor of 2, 4, and 8). Our preliminary results indicated that $\eta$ = 12 dB virtually turned off the system for events of magnitude less than 5, and $\eta$ = 18 dB was not needed. On the horizontal channels, with $\eta$ = 6 dB the detector declared too many false alarms, and with $\eta$ = 12 dB it caught very few events. We were able to modify the vertical channel to give $\eta$ = 6, 9.7, and 12 dB; and $\eta$ = 9.7 dB proved to be very good in our tests.

### 3.4.2 Test Conclusions

From this first round of Alexandria tests (see Table 3-2), we verified the detection criteria for a wide range of events and stations. We discovered that our short-term average did not provide a good turn-off indication, but that the long-term average did. And we learned we could narrow our parameter ranges for $\eta$ and $\tau_{LTA}$ significantly, thereby getting a finer division of the new range for a given number of selectable options. The next modifications to the event detector include the incorporation of a time delay on the turn-on signal to minimize the detector's sensitivity to noise pulses, by ensuring that the STA is greater than $\eta \cdot$ LTA for a certain time lag before declaring an event. The encouraging results of this change, along with a discussion of future topics for investigation, may be found in Section 5. The next section outlines a USO system design using the event detector at this stage of development.

Table 3-2. First Vela test summary.

| Threshold Levels (dB) | 6 | 9.7 | 12 |
|---|---|---|---|
| South of Honshu | | | |
| 10:38:15 MB = 4.5 | | | |
| RKON (86.4) | V | 0 | 00 |
| TFO (86.8) | NA | 0 | 00 |
| Guatemala | | | |
| 10:54:39 MB = 4.1 | | | |
| RKON (37.5) | V | V | NA |
| TFO (27.7) | NA | 0 | 00 |
| California | | | |
| 10:59:17.5 MB = 5.2 | | | |
| RKON (27.4) | V | 0 | 00 |
| TFO (7.9) | X | V | NA |
| Honshu | | | |
| 12:24:08.8 MB = 5.6 | | | |
| RKON (77.4) | X | V | NA |
| TFO (80.0) | X | V | X* |
| California | | | |
| 12:24:35.9 MB = 4.2 | | | |
| RKON (24.8) | NA | 0 | 00 |
| TFO (3.9) | NA | NA | NA |
| E. South Nevada | | | |
| 17:30 Merlin | | | |
| 10 KT | | | |
| RKON (21.0) | X | V | X* |
| TFO (4.8) | X | V | X* |
| Nevada "After Shock" | | | |
| ≈ 17:49** | | | |
| RKON | NA | 0 | 00 |
| TFO | X | V | NA |
| Philippine | | | |
| 17:49:02.9 MB = 5.3 | | | |
| RKON (111.7) | NA | 0 | 00 |
| TFO (110.9) | V | 0 | 00 |

*Very large signal

**Very small signal

†V = detection; X = implied detection; 0 = miss; 00 = implied miss; Time .s GMT; RKON = Ontario; TFO = Tonto Forest; MB = body magnitude, NA = not tested, and numbers in parentheses represent degrees from the source to the receiving station.

SECTION 4

# DETAILED CIRCUIT DESIGN

This chapter will describe the detailed circuit design and analysis undertaken for parts of the USO system described in Section 2. Certain features (the anti-aliasing filters, event detectors, and A/D converter) have been investigated thoroughly, and there exists a high degree of confidence in the proposed approach.

The filter responses and block diagram in Appendices A and B may prove useful in understanding the following discussion.

## 4.1 Anti-Aliasing Filters

Filters are needed to limit the output signals from the six seismometers before sampling for analog-to-digital (A/D) conversion. The information from a sampled input can only be accurately recovered if the input signal bandwidth is limited to one-half of the sampling frequency. Signals greater than this limit produce "aliasing" in the digitized data, hence low-pass filters are used before A/D conversion.

For the long-period seismometers, a five-pole Butterworth low-pass filter will be employed with a -3 dB frequency of 0.1 Hz. This will provide 100 dB of attenuation at the sample frequency of 1.0 Hz (70 dB at 0.5 Hz).

Two possible filters are under consideration for the short-period signals. One is a five-pole Butterworth low-pass filter with a -3 dB frequency of 10 Hz. This filter would provide maximum "flatness" in the passband and a sharp rolloff beyond the break frequency. The other filter being considered is a three-pole Bessel (Gaussian) filter with a -3 dB frequency of 0.8 Hz. This circuit would provide a more linear phase curve than the Butterworth filter, but the rolloff begins at a lower frequency and is not as sharp. The decision of which filter to use will be based on the ease of data-recovery when the tapes are processed.



Preceding page blank

## 4.2 A/D Conversion

The outputs of the aliasing filters are sent to a six-channel time-shared analog multiplexer. Sampling of the long-period data occurs at a 1 sample/second rate whereas the short-period data is sampled at 20 samples/second. When each of these signals is "sampled and held" it goes through the same two-step analog-to-digital (A/D) conversion sequence. We will therefore describe the procedure only once.

The A/D converter will be a 12-bit, dual-slope type with self-calibration circuitry to provide long-term stability. A single-polarity A/D converter currently in use in an operational aerospace system can be used with few modifications. In order to convert both polarities of input voltages, 1/2 of the full-scale voltage will be added to the input prior to conversion. This will provide a digital output of 11 data bits and 1 polarity bit.

In addition to the basic A/D converter, a selectable-gain amplifier will be used to extend the dynamic range of the conversion. A 9-range binary-gain amplifier can extend the dynamic range to 120 dB (the equivalent of a 20-bit A/D converter), while the amplifier gain may be coded easily in 4 bits, so that the total data word is only 16 bits long. (The resolution is still only 12 bits, however.) This is accomplished by a 2-step conversion at each data point. The first conversion determines the binary amplifier gain needed so that the digitized signal is within 6 dB of the full-scale range of the A/D converter for the second conversion. This is analogous to picking the correct scale on a voltmeter: the first reading, done on the lowest scale, determines which scale to use for the second reading to get the most resolution without overloading the meter.

The converter we are considering has a maximum conversion time of 1.6 milliseconds (3.2 milliseconds for our double conversion) allowing 300 words to be digitized each second. We currently use only 63 words per second (and may need 3 more to digitize the long-term averages-LTA) so that the remaining capability may be used for self-calibration. Using this approach, the only component contributing to short-term drift is the zener reference diode in the converter. This would yield a maximum drift rate of about 5 ppm/month.

## 4.3 Event Detector

The event detector consists of three single-channel signal-to-noise ratio comparators and appropriate digital logic to provide an "event duration signal." The "event duration signal" with appropriate prior history, will control the recording of the seismogram.

Each channel of the signal-to-noise ratio detector consists of a gain amplifier, a band-pass filter, full-wave rectifier, short-term averager, long-term averager, signal-to-noise threshold comparator and a sample-and-hold circuit. The band-pass filter is a three-pole Butterworth filter with a passband of two octaves. Using two switches, one can select the center frequency of the filter from three choices. Thus, for the vertical-channel (P-wave) filter a center frequency of 0.5 Hz 1.0 Hz, or 2.0 Hz can be selected. This allows on-site selection of the detection frequency to minimize the effects of background noise at a particular site. With each choice of center frequency, the filter has -3 dB gain points one octave above and below the center with -18 dB/octave (3-pole) rolloffs on each side of the passband. Appendix B represents the actual responses of the filters in our breadboard circuit.

Attempting to get an estimate of the energy in this passband, we use a full-wave rectifier followed by a low-pass filter (the "short-term averager") on the bandpassed signal. The rectifier used in this circuit employs two operational amplifiers and associated diodes and resistors to eliminate the usual problem of 0.6-volt diode drops. Using this precision rectifier, signals under 10 millivolts can be rectified. The second operational amplifier in the rectifier is also used as the short-term averager with an averaging time constant of 1 second. This outputs our STA signal.

The output of the short-term average is then averaged with a longer time constant. This parameter will be site-selectable from 10, 20, 30, or 40 seconds. This signal becomes the "long-term average" (LTA) which is used as our estimate of the background noise.

The basic event detection mechanism is triggered when the ratio of the short-term average (STA) to the long-term average (LTA) exceeds a selected threshold on any of the three channels. This threshold is detected by sensing the polarity of the expression R(STA) - (LTA) where R = 0.5, 0.4, 0.3, or 0.27 corresponding to a "signal-to-noise ratio" (1/R) of 6.0, 7.83, 10.12, or 11.3 dB, respectively. This operation is performed by attenuating the short-term average by the selected factor (R) and comparing this signal with the magnitude of the long-term average.

The assumed cirteria for an event to exist was that the ratio of "signal" (STA) to "noise" (LTA) for one of the channels remained above the selected threshold. However, since the long-term average will build up during an event, this signal does not continue to represent the "background noise," but rather a higher value. It is necessary to freeze the value of the long-term average at the beginning of an event to preserve a true average background noise. Several methods are under consideration for the sample-and-hold circuit which is required to retain the pre-event long-term average. Our current solution to this problem is to use a counter, D/A converter, comparator and three-channel multiplexer to hold the LTA of the channel which triggers first.

When one of the signal-to-noise ratio detectors indicates an event, the analog multiplexer feeds the long-term average of the triggered channel to the input of the sample-and-hold. The output of the sample-and-hold is continuously compared with the current LTA, and the event is considered "over" when the long-term average returns to its pre-event level (retained by the sample-and-hold). To avoid recording too long after the end of an event, we wanted to store a slightly higher value in the sample-and-hold than the LTA at the instant an event began. Ideally, we would have amplified the LTA by a fixed gain just before storage, but this proved impractical in the development time available. As an alternate approach, used in our testing program, we waited 1 or 2 seconds after an event was triggered, letting the LTA build up, before storage. The obvious drawback to this scheme is that during a false alarm, when no event is present, the LTA does not build up, and the system waits too long before shutting off the recorder.

The simulated operation of the event detector is shown in Figure 4-1. There would be one such detector on each short-period seisomometer output.

## 4.4 30-Second Buffer Memory

In order to preserve the beginning of an event while the detector takes time to respond, we plan to pass all short-period data through a digital delay line in the form of a static shift register. The data arrives as 16-bit words from the A/D converter. Each of the three channels produces 20 words per second, so that 960 bits per second are fed to the shift register. A 30-second delay line was felt to be sufficient for our needs, so that a 28,800-bit shift register would be required.

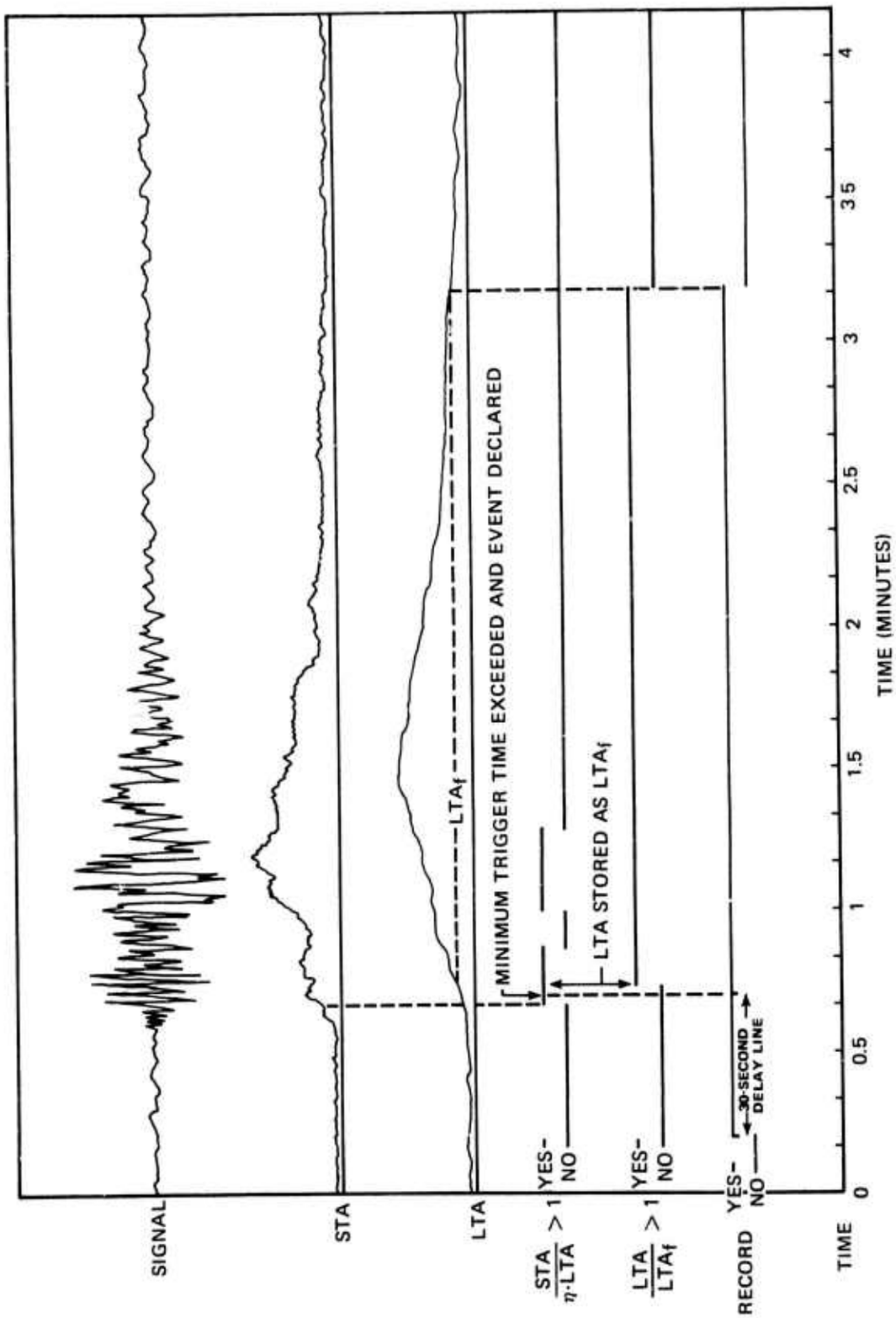



Figure 4-1. Simulated event detector operation.

For high reliablilty and low power, we planned upon using MOS (metal oxide semiconductor) memory elements, preferably CMOS (Complimentary MOS). CMOS registers, while offering a two-order-of-magnitude savings in power, are currently only available in 64 bits-per-package sizes, while the MOS type may be found, at much lower cost, in 1024-bit packages.

We investigated the feasibility of placing 16 CMOS devices (a 64-bit RCA type) in a single package, and three manufacturers were contacted for price quotations. Appendix C contains a copy of the letter sent to RCA, Halex Inc., and ILC Data Device Corp., along with a summary of their replies. RCA provided the lowest volume-per-bit ratio and the lowest cost in quantity production.

A summary of our component comparisons is given in Table 4-1. The first entry is a MOS 1024-bit package, and 29 units would be needed for the memory. The second and third entries are smaller capacity CMOS devices, with many more being needed for the system. The fourth component is an RCA packaging of their own devices. The final decision would seem to be between the first and fourth packages. The second and third entries have costs within 25 percent of that of the fourth device, but require many more assembly and test operations (in final assembly).

## 4.5 Station Timekeeping

Timing information will be vital to the interpretation of the recorded seismic data from the USO. We plan to use a temperature-compensated crystal oscillator as the primary clock for the entire station. Such clocks typically have frequency drifts of less than 1 part in $10^7$ per day, accomplishing this without the added power usage of a temperature-controlled oven. In addition to an accurate frequency standard, accurate station time (and time synchronous with other USO stations) would seem to require that provision be made for occasional clock updating.

## 4.6 Tape Recorder

Two identical tape recorders will be employed at each USO to provide a continuous, permanent data record. Only one recorder will be operated at any one time, recording all long-period data and all short-period events, along with an occasional station ID and time code.*

* The authenticator circuit developed by Sandia Corp. may make provisions for time information once in every 1024 bits of data. If this authenticator is used, we will schedule the time codes accordingly. This area will be discussed further in our following report.

Table 4-1. 30-second memory component comparison.

| Device | Power Supplies Required (V) | Temp. Range ($^{o}$C) | Package | Bits/ Package | No. of Devices Required | Total Area (in$^{2}$) | Total Power (watts) | Cost Rating (based on 22 USO systems) |
|---|---|---|---|---|---|---|---|---|
| 1. Signetics Z533 (MOS) | + 5<br>-12 | 0 to +70 | 8-pin chip | 1024 | 29 | 3.4 | 4.2 | Lowest |
| 2. Motorola MC14517AL (CMOS) | + 5 | -55 to +125 | 16-pin dual in line | Dual 64 | 225 | 57.0 | 0.04 | High Middle |
| 3. RCA (CMOS) CD 4031AK | + 5 | -55 to +125 | 16-lead flat package | 64 | 450 | 99.0 | 0.04 | Low Middle |
| 4. RCA (CMOS) CD4031AH | + 5 | -55 to +125 | 16 CMOS chips/package | 1024 | 29 | 29.0 | 0.04 | Highest |

The second recorder will be used when the first is malfunctioning or out of tape. During this period, the tape may be changed on the first unit without loss of any data.

The data words themselves provide timing information, with each long-period block (3 words: 1 per channel) indicating a 1-second time increment. Similarly, the number of short-period 3-word blocks until the next long-period block indicates the start time of short-period recording (displaced exactly 30 seconds by the delay line) to the nearest 0.05 seconds (20 blocks-per-second sample rate).

## 4.7 Power Budget

The power budget is summarized in Table 4-2. It covers the event detector electronics located down-hole and is predicted to be approximately 2.4 watts. This assumes that the 30-second buffer memory for short-period data consists of CMOS devices; if Signetics-type MOS memory is employed, the predicted power consumption will be approximately 7.5 watts. This does not appear to create undue heat-dissipation problems down-hole.

## 4.8 Summary

This chapter, in conjunction with the block diagram and circuit diagrams in the appendices, has described our event detector design. We have also outlined the more important components of the USO that need to be assembled to complete a station design. Table 4-3 summarizes the characteristics of our design at this stage of development.

Table 4-2. USO event detector power budget down-hole (watts).

| FUNCTION | +5 Volts | | +15 Volts | | -15 Volts | | TOTAL |
|---|---|---|---|---|---|---|---|
| | TYP | MAX | TYP | MAX | TYP | MAX | |
| (1) Aliasing Filters | | | | | | | |
| (a) 3 long period | | | 0.041 | 0.108 | 0.041 | 0.108 | 0.082 |
| (b) 3 short period | | | 0.041 | 0.108 | 0.041 | 0.108 | 0.082 |
| (2) 3 wave Discriminators | | | 0.110 | 0.290 | 0.110 | 0.290 | 0.220 |
| (3) 12-bit A/D Converter | 0.001 | 0.010 | 0.195 | 0.275 | 0.180 | 0.261 | 0.375 |
| (4) 30-second Buffer Memory | 0.04 | 0.50 | | | | | 0.040** |
| (5) Memory-D/A Converter | 0.01* | | 0.040* | | 0.010* | | 0.06 |
| (6) Analog Multiplexer | | | 0.025 | 0.03 | 0.025* | 0.03 | 0.05 |
| (7) Timing Logic | 0.80* | | | | | | 0.80* |
| (8) Control Logic | | | | | | | |
| (9) Power Converter | 0.25* | | 0.060* | | 0.057* | | 0.367* |
| (10) Digital I/O Section | 0.10* | | | | | | 0.10* |
| (11) Discriminator Decode Logic | 0.10* | | | | | | 0.10* |
| (12) Crystal Oscillator | 0.10* | | | | | | 0.10* |
| Known | 0.041 | | 0.387 | | 0.371 | | |
| Projected | 1.36 | | 0.125 | | 0.092 | | |
| Total | 1.401 | | 0.512 | | 0.463 | | 2.376 W |

*Projected power values

**CMOS

Table 4-3. Performance characteristics of the event detector.

| | | | |
|---|---|---|---|
| (1) | Seismometer Interface | | |
| | (a) | Low noise devices and appropriate ground transfer to be employed. | |
| (2) | Anti-Aliasing Filter | | |
| | (a) | Long period | |
| | | (i) Type | 5th order Butterworth |
| | | (ii) Break frequency | 0.1 Hz |
| | | (iii) Passband ripple | $<\pm 3$ dB |
| | (b) | Short period | |
| | | (i) Type | 5th order Butterworth |
| | | (ii) Break frequency | 10 Hz |
| | | (iii) Passband ripple | $\leq \pm 3$ dB |
| (3) | Analog-to-Digital Converter | | |
| | (a) | Type | Dual slope integration with self calibration |
| | (b) | Number of bits | Sign plus 11 binary bits |
| | (c) | Conversion time | 1.6 ms |
| (4) | Binary Gain Amplifier | | |
| | (a) | Dynamic range | 60 dB |
| | (b) | Coded bits | 4 |
| | (c) | Ranges | 9 |
| (5) | Conversion Rates | | |
| | (a) | Long-period data | 3 long-period signals converted once/second |
| | (b) | Short-period data | 3 short-period signals converted 20 times/second |
| (6) | Short-Period Memory | | |
| | (a) | Components | MOS/CMOS |
| | (b) | Delay capability | 30 seconds |
| | (c) | Total no. of bits | 28,800 bits |
| | (d) | Type | static-shift register |

Table 4-3. Performance characteristics of the event detector (continued).

| | | | |
|---|---|---|---|
| (7) | Short-Period Event Detector | | |
| | (a) | Gain amplifier site-selectable from 10 to 1000. | |
| | (b) | Independent long-term averager selectable from 10 to 40 seconds. | |
| | (c) | Independent threshold comparator selectable from 6 to 12 dB. | |
| | (d) | Independent narrow-band frequency select capability 0.5, 1, and 2 Hz for the vertical channel. | |
| | (e) | Independent narrow-band frequency select capability of 0.25, 0.5, and 1 Hz for the 2 horizontal channels. | |
| | (f) | Selected channel freezes background noise in a digital manner. | |
| | (g) | STA/LTA ratio to exceed comparator threshold for a minimum of 1 2 to 2 seconds in order to minimize the false-alarm rate. | |
| | (h) | Turnoff (end-of-event signal) controlled by frozen background noise (LTA) and continually integrated long-term average of the tripped channel. | |
| | (i) | 30 seconds of background noise prior to the start of an event is recorded. | |
| | (j) | Automatic reset of end-of-event signal after 8 minutes of recording short-period data. | |
| (8) | Data Transmission | | |
| | (a) | Type | Serial data bus |
| | (b) | Rate | Dependent on recording system |
| (9) | Crystal | | |
| | (a) | Stability | 1 part in $10^7$ per day |
| | (b) | Usage | Primary clock for the entire system |
| (10) | Power | | |
| | (a) | Voltages | 4 selected regulated voltages for the event detector system and remaining subsystems |
| | (b) | Power | 2.4 to 7.5 watts depending on the choice of 30-second memory type |

# SECTION 5

# SECOND SERIES OF TESTS AT VELA

We returned to the Vela Seismological Center in the middle of October 1973, to test our event detector design with the modifications described at the end of Section 3. The earlier Vela tests had shown that the ranges of the selectable time constants and threshold values could be narrowed. The tests also implied that certain small modifications might significantly reduce the false-alarm rate, particularly on the horizontal channels. These modifications were included in the design discussed in Section 4.

## 5.1 System Modifications

The principal modification to the detection function was the introduction of a delay circuit after the triggering signal. The STA/LTA comparator output would have to remain above the threshold $\eta$ for a specified time interval (0 to 4 seconds) before the detector would declare an event. This feature proved very useful in lowering the false-alarm rate without harming our chances of detecting a true event.

We also incorporated a feature to decrease the amount of time that the detector would be "on" for each event (the amount of data which the detector would consider worth recording). As discussed earlier, the detector would signal a "turnoff" when the LTA (long-term average) was near its pre-event level. This would not happen until long after an event was over, and we wanted to avoid taping the whole recovery period of the LTA. Ideally, therefore, we would store a higher value (e.g., $K \cdot LTA$ where $K > 1$) than the pre-event LTA and then compare the current LTA to this stored level in order to turn off a little earlier. This scheme, however, was too hard to implement in the time available.

Instead, we were able to perform a similar amplification of the LTA simply by waiting from 1 to 4 seconds after an event was declared before sampling and storing. This let part of the event energy into the LTA, causing it to read a higher value than the pre-event background



Preceding page blank

noise. The drawback to this method is that, when triggered by a false alarm, the LTA will not rise as expected, and the system will wait a long time for a small decrease in the background noise to bring the LTA below its ambient level. Although this scheme (delay before storing) did prove useful in evaluating the turn-off criterion it may still be replaced by an alternate one (amplification before storing) in an operational system.

With these modifications, the prototype was returned to Vela for further testing. The test setup was the same as before (see Section 3), and the results are given below. (Examples of Vela data may be found in Appendix D.)

## 5.2 Test Results

### 5.2.1 Band-Pass Filters

The band-pass filters we used were all three-pole Butterworth types with -3 dB frequencies at $\pm$1 octave from the center frequency. We chose center frequencies of 1 Hz for the vertical channel filter and 1/2 Hz for the horizontal channels, as explained in Section 3. We also incorporated alternate band-pass filters as "site-selectable" options in our final design. The center frequencies for the alternate filters (two per channel) were one octave above and below the nominal center frequency for that channel. While the nominal values proved satisfactory in all of our tests, we still recommend that the alternate values be included in a remote station to adapt the detector to individual site peculiarities.

On one occasion during our tests, the band-pass filters particularly proved their worth. We were testing the detector on a very large earthquake "swarm" in the Aleutians (during February 1965), as recorded at an Aleutian Observatory (Adak Island). The (long-period) surface waves were still visible on the short-period channels long after the short-period waves had subsided. The band-pass filters allowed the detector to trigger on an early P wave, shut off after the wave died down, and trigger again when a second body wave phase (or reflection) was seen. Since the long-period waves would be continually recorded in our station design (see Section 2), this short-period selectivity in the detector is very desirable.

### 5.2.2 Energy Averages

In our tests, we used a time constant of 1 second for the short-term average (STA). This low-pass filter appeared to respond quickly to the "front" of the seismic wave, without passing excessive ripple from the rectification of the wave itself.

The long-term average (LTA) time constant had been set at 50 seconds for the early digital computer simulations of our detector design. This provided an adequate noise estimate for good detection. Alternate time constants of 120 and 10 seconds were included as comparisons, but they appeared unsatisfactory. The 120-second filter took too long to recover from an event so that the detector sensitivity to new events was decreased immediately following a large event. On the other hand, the 10-second filter reacted too quickly, and while it recovered from a large event in a reasonable time, it was not different enough from the STA time constant to provide a good detection criterion.

The modification to our design which compared the LTA to the frozen LTA for a turn-off indication put new constraints on our time constant choice. The 50-second time constant was too long for this scheme because it caused us to record for too long after each trigger. We therefore investigated the range from 10 to 50 seconds. The second Vela test series showed that 37 seconds would cause too much recording on big events, while 10 seconds seemed to hurt the probability of detecting slowly-emerging (no definable wave-front) events. Our nominal value of 20 seconds appeared to be the best compromise, but again we recommend including alternates (from 10 to 40 seconds) to compensate for site peculiarities.

### 5.2.3 Threshold Levels

The original range of threshold values for our test was 6, 12, and 18 dB (factors of $\eta$ = 2, 4, and 8, respectively). Our first tests at Vela indicated that 6 dB could be used for a very good vertical channel seismometer without creating too many false alarms, while 12 dB was high enough to virtually turn off the detector, letting it detect only the largest of the real events. On the horizontal channels, a 6-dB threshold yielded too many false alarms for most cases (except where our pulse-smoothing was effective – see below), while 12 dB was also too high to be effective.

Our final breadboard design used four values between 6 and 12 dB, and aside from the expected reduction in triggering rate associated with the higher values, all values appeared useful for some sites. We therefore recommend the inclusion of the full 6- to 12-dB range in any operational system, with at least four choices in that range for on-site "fine tuning".

### 5.2.4 Digital Smoothing

The first Vela test series revealed a large number of false alarms on the horizontal channels at the 6-dB threshold setting. Most of these false triggers lasted less than a second, while real events tended to provide a longer-lasting trigger. Thus, we thought that a "smoothing" circuit – one that only declared an event if a channel triggered (STA/LTA > η) for longer than a preset interval (0 to 4 seconds) – would help reduce the false-alarm rate.

The test configuration for the second Vela series incorporated this feature on all three channels. The most significant improvement occurred in the horizontal channels, where false alarms had been more of a problem. This preset interval before declaring an event may be called the "minimum trigger time". The following paragraphs describe the effect of this smoothing method on our detector for an 8-minute section of tape from the second Vela series.

The results of testing the horizontal detectors on a tape made at Tonto Forest of an event (S-wave) at Honshu, Japan* are shown in Table 5-1. The results indicate that at a 6-dB threshold level, many false alarms were generated when no minimum trigger time was used. Increasing the minimum trigger time to 1/2 second kept any false triggers from being regarded as events. Increasing the threshold to 8 dB kept any false triggers (and therefore events) from being generated.

Increasing the minimum trigger time beyond 1 second did not appreciably reduce the false-alarm rate further. Indeed, a 4-second minimum prevented the detection of a few real events. The optimum improvement seemed to occur between 1/2 and 1 second, and we recommend that this range be investigated more thoroughly.

---

*All channels detected the actual event in this section of tape, a Honshu earthquake on 12/16/65 at 12:24 08.8 GMT $M_{body}$ = 5.60, Δ = 80.0.

Table 5-1. Total number of false triggers and events on both horizontal event-detector channels from an 8-minute tape section.

| Run No. | Threshold Level (dB) | Minimum Trigger Time (s) | $\tau_{LTA}$ (s) | No. of False Triggers | No. of False Events | Record Time* (s) |
|---|---|---|---|---|---|---|
| 1 | 6 | 0 | 20 | 10 | 7 | 38 |
| 2 | 6 | 1/2 | 20 | 8 | 0 | 35 |
| 3 | 6 | 1/2 | 30 | 9 | 0 | 38 |
| 4 | 8 | 0 | 20 | 0 | 0 | 34 |
| 5 | 8 | 1/2 | 20 | 0 | 0 | 17 |
| 6 | 8 | 1/2 | 30 | 0 | 0 | 33 |

*Recording time for the real event, not including 30-second delay-line coverage. The event contained about 10 seconds of useful information.

5.2.5 Event Duration

We investigated the effects of various parameters on the amount of data the detector deemed worth recording for each event (event duration). Figure 5-1 illustrates the results of a series of tests made on the recording of a Nevada underground nuclear explosion as seen at Tonto Forest Observatory ($\Delta = 4.8°$).*

The results, in general, confirmed our expectations. Increasing the threshold resulted in turning off earlier, and for each set of parameters, the threshold-increasing sequences stand out. Increasing $\tau_{LTA}$ to 30 seconds increased the amount of time we recorded. Increasing the minimum trigger delayed the declaring of an event until after the LTA had build up slightly, so that the turnoff occurred earlier.** The sample-delay (before freezing the LTA) had the same effect of shortening the event duration. As mentioned earlier, this feature may be replaced in our final design by one which multiplies the $LTA_{frozen}$ by a turn-off threshold to achieve a similar amplification. For these tests, where an event is present, increasing the LTA sample-delay is similar to increasing the turn-off threshold.

*Event called "Merlin" on February 16, 1965 at 17:30 GMT.

**This factor is most useful for minimizing false alarms.

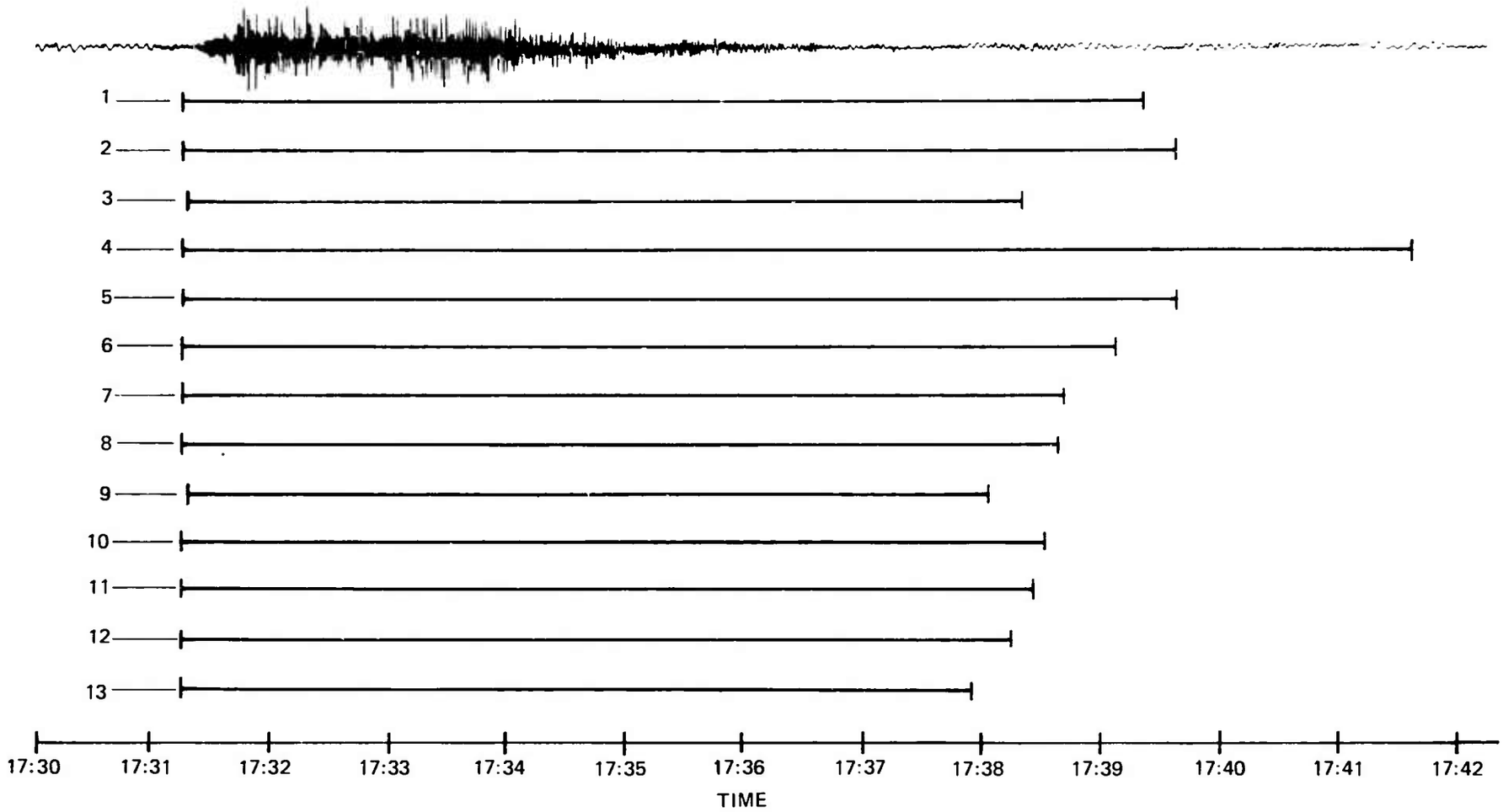



Figure 5-1. Event detector recording time (without 30-second pre-event memory) for parameters listed in Table 5-2.

### 5.2.6 Simultaneous Three-Axis Operation

After fine tuning the event detector (through the site-selectable parameter options) (Table 5-2), we ran a series of tests on three-channel data from various recording locations. These tests investigated the interactions between the three channels as well as their relative strengths and weaknesses.

Table 5-2. Effects of parameter changes on the duration of the recording command.

| Run No. | η(dB) | $\tau_{LTA}$ (s) | Minimum Trigger Time (s) | Sample-Delay (s) | Event Start (h:min:s) | Duration (min:s) |
|---|---|---|---|---|---|---|
| 1 | 6 | 20 | 0 | 1 | 17:31:15 | 8:7 |
| 2 | 8 | 20 | 0 | 1 | 17:31:15 | 8:23 |
| 3 | 10 | 20 | 0 | 1 | 17:31:17 | 7:05 |
| 4 | 6 | 30 | 0 | 1 | 17:31:15 | 10:23 |
| 5 | 8 | 30 | 0 | 1 | 17:31:15 | 8:23 |
| 6 | 10 | 30 | 0 | 1 | 17:31:15 | 7:53 |
| 7 | 6 | 20 | 0 | 2 | 17:31:15 | 7:28 |
| 8 | 8 | 20 | 0 | 2 | 17:31:15 | 7:27 |
| 9 | 10 | 20 | 0 | 2 | 17:31:16 | 6:48 |
| 10 | 6 | 20 | 1/2 | 1 | 17:31:15 | 7:17 |
| 11 | 8 | 20 | 1/2 | 1 | 17:31:15 | 7:12 |
| 12 | 10 | 20 | 1/2 | 1 | 17:31:16 | 6:57 |
| 13 | 11 | 20 | 1 | 4 | 17:31:15 | 6:40 |

Three types of responses were particularly noteworthy. First, for large events located close to the recording station, the vertical and horizontal channels would trigger on their respective components of the P-wave. Thus, for the close-in events of interest to the USO program, the horizontal channels would act as a backup to provide detection "insurance". Second, for smaller nearby events, or periods when the horizontal thresholds had been set relatively high, the vertical channel would trigger on the P-wave and the horizontal channel would trigger on the slightly delayed S-wave (due to its larger amplitude). This again acted as a backup, since the horizontal channel triggers would occur while the 30-second buffer memory still remembered

the initial motion on all three channels. Third, on distant teleseisms (where the S-wave would arrive minutes after the P-wave motion had subsided), the vertical channel would detect the P-wave and the horizontal detectors would spot the separate, delayed S-wave. (In addition, the horizontal channels would occasionally trigger on the horizontal component of the P-wave, again providing a backup.) These test results indicate that the three detectors would complement and reinforce one another, resulting in a reliable system for the detection of seismic waves on any channel. (In Appendix D, an example of three simultaneous triggers is shown in Figure D-2; delayed horizontal triggers appear in Figure D-4.)

We had originally envisioned three completely independent detector circuits, whereby each channel would generate an event-duration signal. The system would record as long as at least one of the three signals indicated an event. This method required remembering (freezing) the pre-event noise level of any channel that triggered. Our prototype, however, had only one event-duration signal derived from the first channel which triggered for a particular event. The only time that our prototype arrangement would be inferior to the original scheme would be when multiple channels triggered on the same event and the first channel shut off while useful data existed on another channel.

From our tests, we feel that any channel that triggers would usually provide a reliable turn-off signal for all three channels. It appears that the two systems would perform nearly identically, and that the prototype design, being the easier of the two to implement, may be the better choice. This area should, however, be analyzed in detail to verify these impressions and further justify the use of the simpler design.

## 5.3 Discussion of Results

The results of the two series of Vela tests were very encouraging. The event detector appears capable of detecting nearby events as well as the multiple phases of teleseisms, while maintaining a very low false-alarm rate. The device was easily adaptable, by means of the site-selectable parameters, to a variety of seismometer locations as represented by their recorded signals.

We have refrained from quoting numbers for our performance characteristics (e.g., body magnitudes of detectable events, or false-alarm probabilities) because we have not yet field-tested the instrument. The detector, while maintaining a very low false-alarm rate, was able to detect virtually all of the events that we could discern on the seismogram as played back. The original data had been recorded on magnetic tape (through frequency-modulation techniques) at the receiving observatory and was then played back, in a somewhat noisier form, at Vela. The result was that the test apparatus appeared to limit our performance, and while we were pleased with our design, we must reserve final judgment until the completion of field testing.

## SECTION 6

## CONCLUSION

We have developed an analog seismic event detector and outlined the design of an unattended seismic observatory in which the detector would be quite useful. While it is impossible to provide all of the test data and to detail fully our design evolution, we have tried to describe the major factors influencing our final design. From our experience in testing the event detector prototype, we have developed a great deal of confidence in this design and its usefulness.

We feel, however, that certain additional work should be performed. The most important task remaining is the field testing of the prototype event detector with actual seismometers. Only in this way can we verify our performance characteristics. In addition to the field tests, certain topics need further investigation. These features include: an investigation of the "minimum trigger time" used to reduce the false-alarm rate, an examination of the turn-off criterion using an amplified, rather than delayed, long-term average (LTA) to reduce the recorded data, and an analysis of a detector using three fully independent turn-off criteria, rather than the single-channel turn-off used in our prototype. This future effort, in conjunction with our current design, should provide a useful, economical system for remote event detection.

# APPENDIX A

## EVENT DETECTOR SCHEMATIC

SITE-SELECTABLE PARAMETERS

Table A-1. Center frequency of band-pass filter.

| Desired Center Frequency (Hz) | | Switch States | |
|---|---|---|---|
| Vertical | Horizontal | $f_o$-1 | $f_o$-2 |
| 0.5 | 0.25 | Closed | Open |
| 1.0 | 0.5 | Open | Open |
| 2.0 | 0.1 | Open | Closed |

Table A-2. Time constant of the long-term averager.

| Desired Time Constant (s) | Switch States | |
|---|---|---|
| | $\tau_N$-1 | $\tau_N$-2 |
| 10.2 | Open | Open |
| 20.4 | Closed | Open |
| 30.6 | Open | Closed |
| 40.8 | Closed | Closed |



Preceding page blank

Table A-3. "Signal/noise" threshold level.

| Desired S/N Threshold (dB) | Switch States | |
|---|---|---|
| | S/N-1 | S/N-2 |
| 6 | Open | Open |
| 7.83 | Closed | Open |
| 10.1 | Open | Closed |
| 11.3 | Closed | Closed |

Table A-4. Channel-dependent values.

| Component | Vertical | Horizontal |
|---|---|---|
| R10 | 18k | 36k |
| R12 | 56k | 110k |
| R14 | 51k | 100k |
| R15 | 110k | 220k |
| R17 | 300k | 680k |
| R19 | 330k | 620k |
| R20 | 330k | 620k |
| R21 | 910k | 2.0M |
| R23 | 470k | 1.0M |
| R25 | 620k | 1.2M |
| R26 | 82k | 160k |
| R28 | 75k | 160k |
| R30 | 27k | 51k |
| R31 | 820k | 1.6M |
| R34 | 820k | 1.6M |
| R37 | 1.6M | 3.3M |

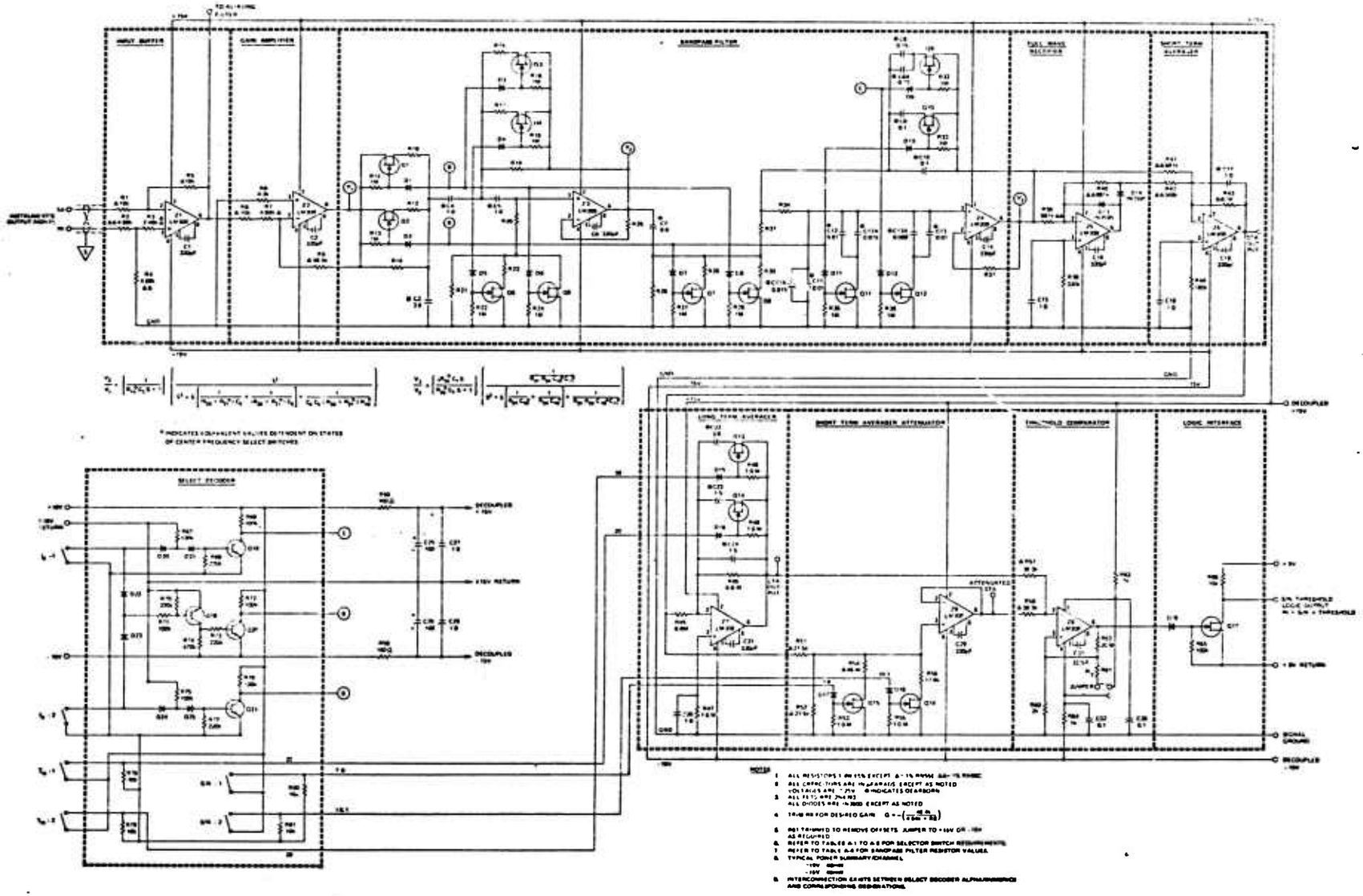


Figure A-1. Single-channel event detector.

# APPENDIX B

## BAND-PASS FILTER FREQUENCY RESPONSES

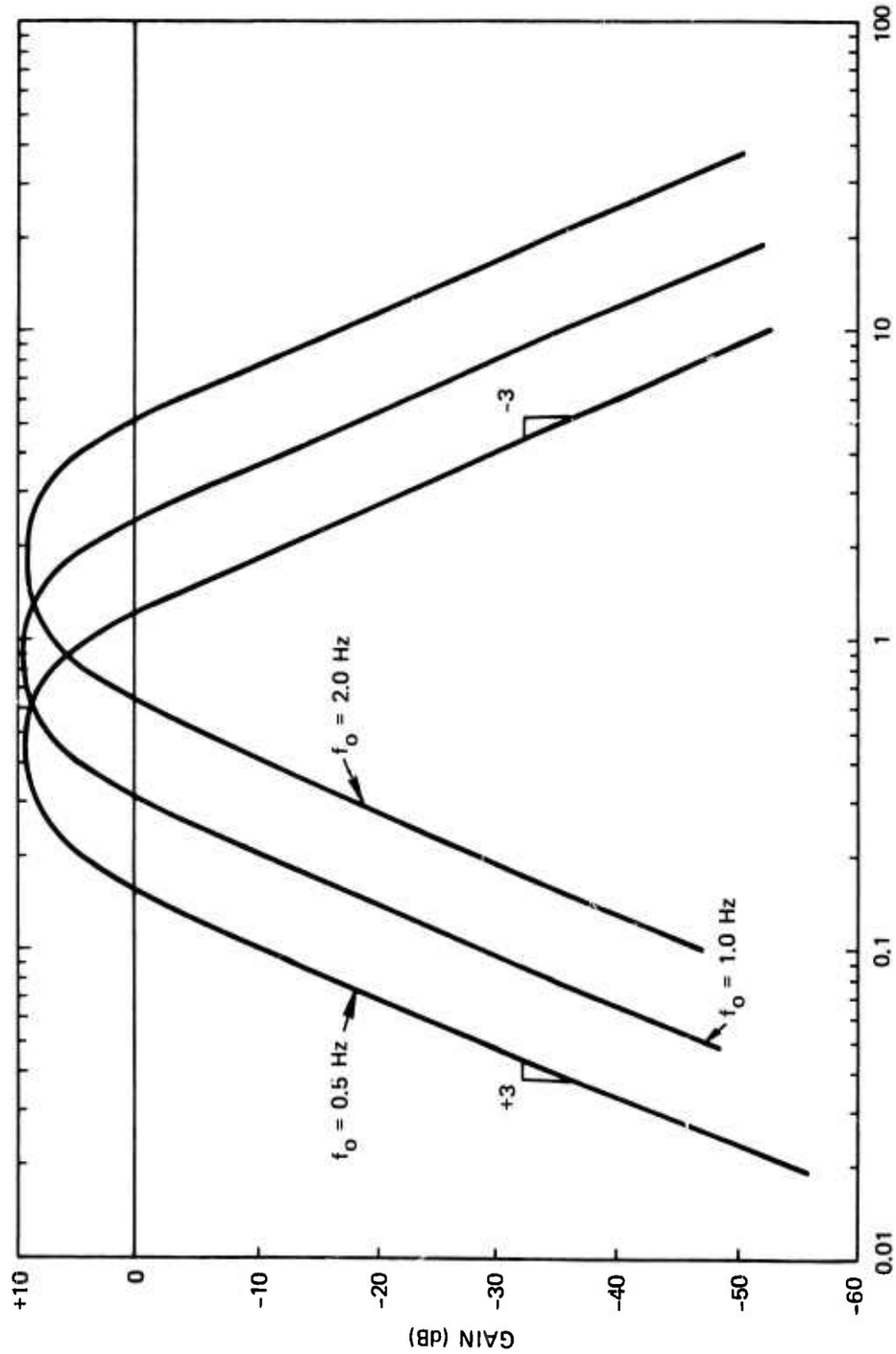



Figure B-1. Vertical-channel band-pass filter options.

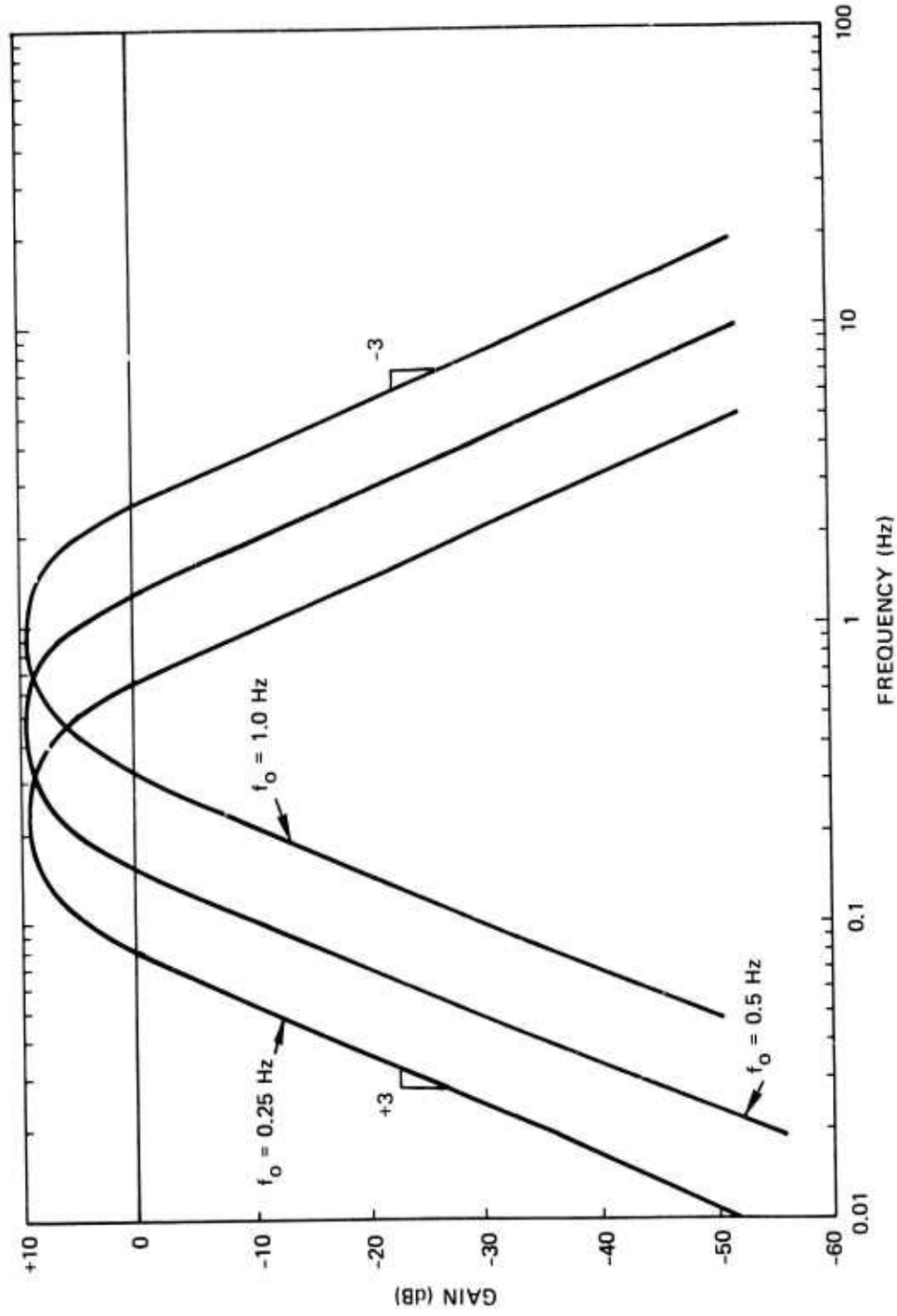



Figure B-2. Horizontal-channel band-pass filter options.

# APPENDIX C

## 30-SECOND MEMORY QUOTE COMPARISON

(1) RCA, Burlington, Mass.

Package size - 1 x 1 x 0.13"
Bits/package - 1024
Cost/quantity

(a) 37 - Highest
(b) 337 - Lowest
(c) 625 - Lowest

(2) Halex, Inc.

Package size - 1 x 1 x 0.16"
Bits/package - 512
Cost/quantity

(a) 74 - Lowest
(b) 674 - Middle
(c) 1250 - Middle

(3) ILC Data Device Corp.

Package size - 0.9 x 1.65 x 0.14"
Bits/package - 1024
Cost/quantity

(a) 37 - Middle
(b) 337 - Highest
(c) 625 - Highest

Following is an example of a letter requesting packaging information (used for above comparison).



Preceding page blank

Larry J. Freier DL6-310 MS #88
The Charles Stark Draper Laboratory, Inc.
68 Albany Street, Cambridge, Massachusetts 02139 Telephone (617) 258-3494

August 24, 1973

H. C. Center
RCA Aerospace System Division
Burlington, Mass.

Dear Mr. Center:

This letter constitutes a followup of my conversation with Mr. B. T. Joyce on 24 August 1973. It is requested that RCA submit a quote for the manufacture of single packaged devices which will contain 16 RCA 64-bit shift register (CD4031AH). Such a final device could provide 1024 bits of static shift register capability.

It should contain the following input/output terminals:

1. Data In
2. Mode Control
3. Recirculation In
4. Clock Input
5. Relayed Clock Output
6. $V_{DD}$
7. $V_{SS}$
8. Q Output
9. $\overline{Q}$ Output

Electrical performance characteristics contained within RCA Solid State Data Book 203A, p. 152-157 are applicable.

Your quote should contain the following:

1. A description which presents your previous background experience in this area of fabrication.
2. Your proposed manner of manufacturing the device.

3. Your method of inspection and checkout of the device and to what standard.

4. Proposed package dimensions and configuration.

It is requested that you provide a quote for three separate quantities. Within each of the three, a separate cost breakout should exist for manufacture and final component checkout. The purchase of chip parts from RCA will be your responsibility. The three quantity breakouts are as follows:

a. 37 - 1024 Static Shift Registers

b. 337 - 1024 Static Shift Registers

c. 625 - 1024 Static Shift Registers

If there is any additional information you require please contact me. Your prompt response to this letter will be greatly appreciated.

Yours truly,

Larry J. Freier

Telephone #617-258-3494

# APPENDIX D

## DATA FROM VELA TESTS



Preceding page blank

This appendix contains five recordings from our Vela test program. The seismograms from two nuclear tests (in southern Nevada) are shown from each of two receiving observatories along with an uncataloged event detected after one of the explosions. The nuclear tests were "Cashmere", which occurred at 15:30 GMT on February 4, 1965, and "Merlin", which occurred at 17:30 GMT on the 16th of the same month. Following Merlin (by about 10 minutes), an uncataloged event occurred which was only observable at the closer of the two stations. The two stations used here are RKON (Ontario) and TFO (Tonto Forest Observatory). Both explosions occurred 21.0° from RKON and 4.8° from TFO. The events are shown in the following order:

(1) "Cashmere" recorded at RKON
(2) "Cashmere" recorded at TFO
(3) "Merlin" recorded at RKON
(4) "Merlin" recorded at TFO
(5) Uncataloged event recorded at TFO

Remarks

- The recordings were made with light pens, and the channels were allowed to overlap to provide better resolution for each channel (at the expense of clarity).
- The STA and LTA channels all have reference (0) lines. The STA is read positive below its reference; the LTA positive above its reference.
- The "comparator" reads "high" when STA/LTA > η, and "low" otherwise.
- The "record signal" reads "high" when the data is to be recorded, and "low" otherwise, with one exception: 30 seconds of data immediately preceding the recorded section shown here would be recorded in the final design (from the buffer memory). This is shown in Figure 4-1.



Preceding page blank

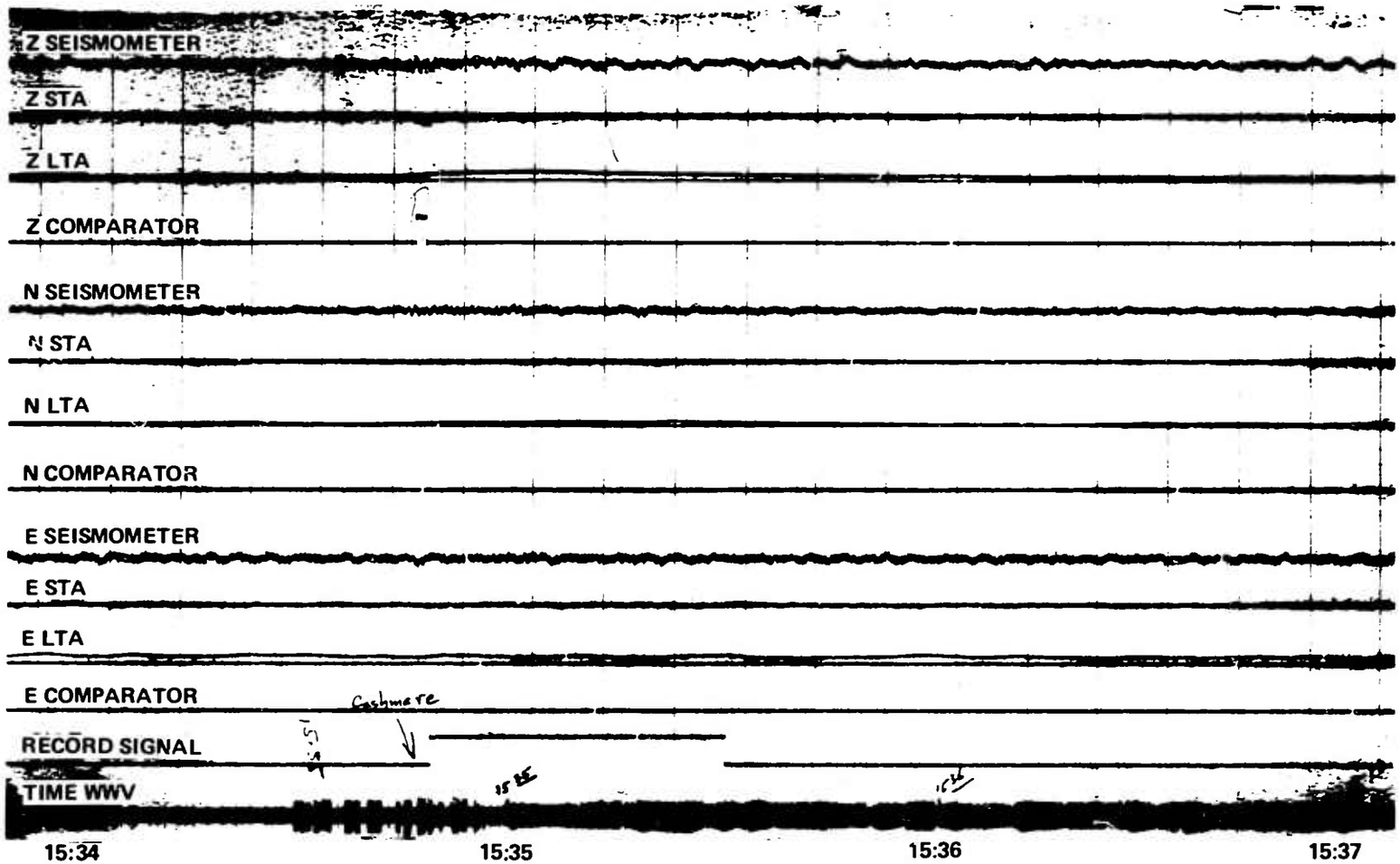



Figure D-1. "Cashmere" recorded at RKON.



Preceding page blank

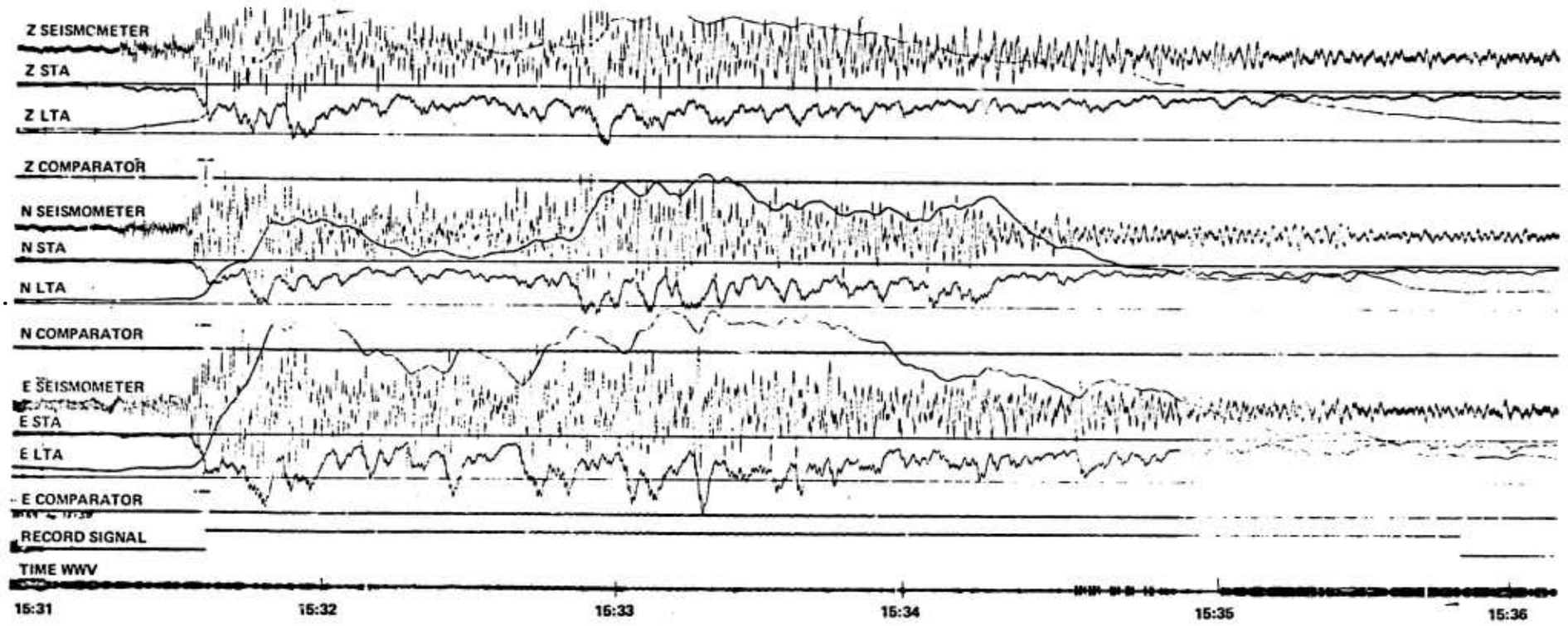



Figure D-2. "Cashmere" recorded at TFO.



Preceding page blank

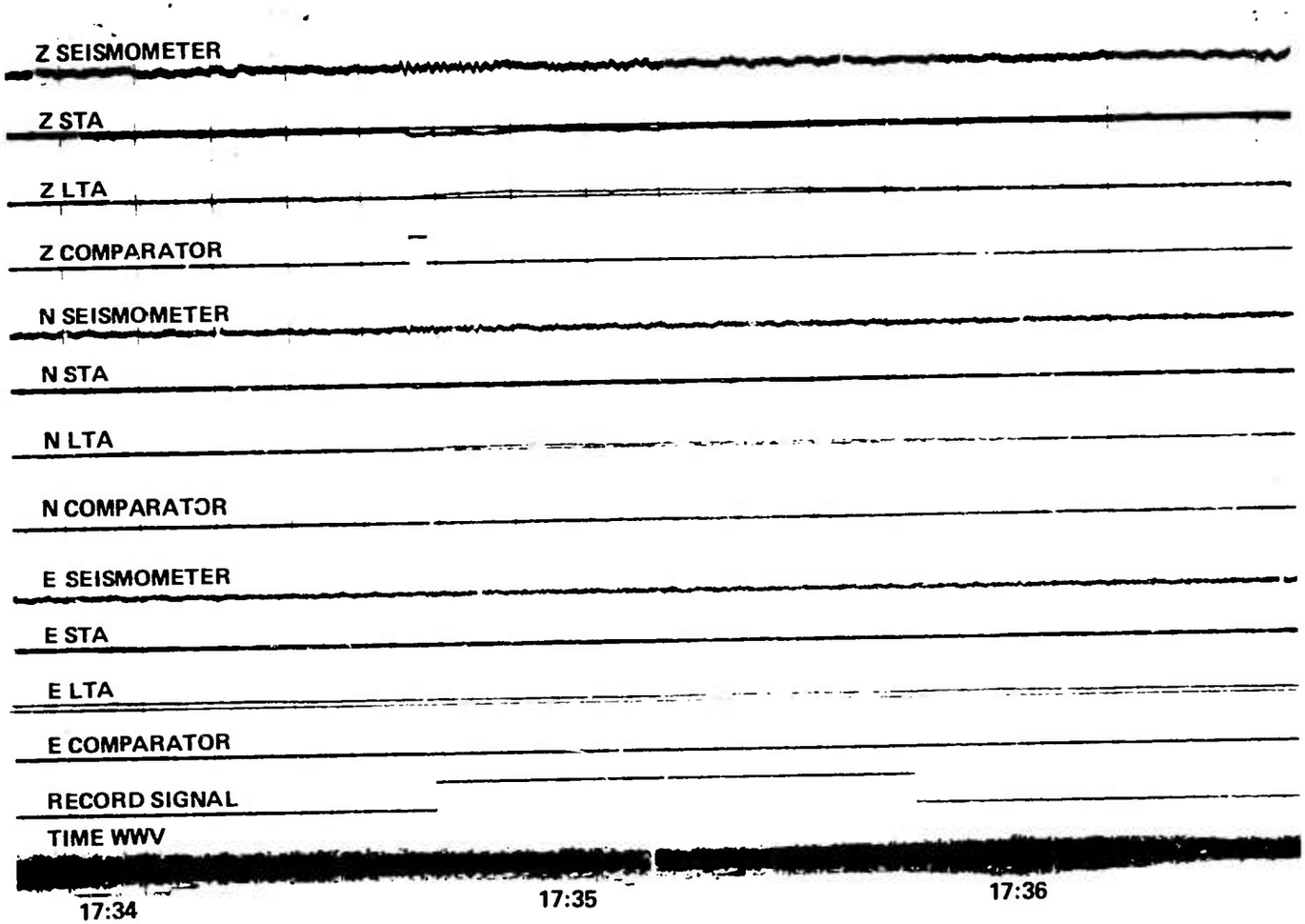
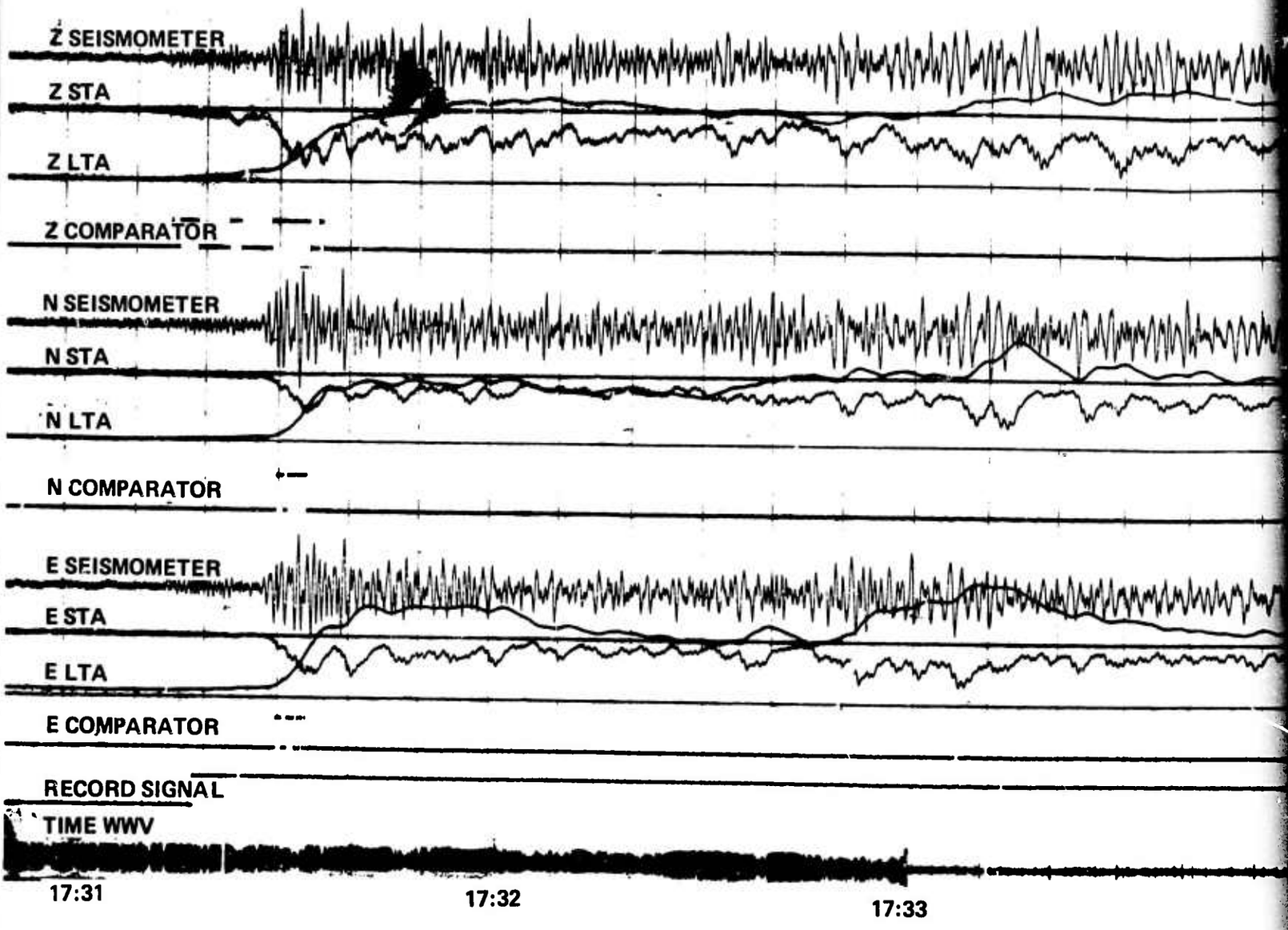



Figure D-3. "Merlin" recorded at RKON.



Preceding page blank


Z SEISMOMETER
Z STA
Z LTA
Z COMPARATOR
N SEISMOMETER
N STA
N LTA
N COMPARATOR
E SEISMOMETER
E STA
E LTA
E COMPARATOR
RECORD SIGNAL
TIME WWV
17:31
17:32
17:33

A

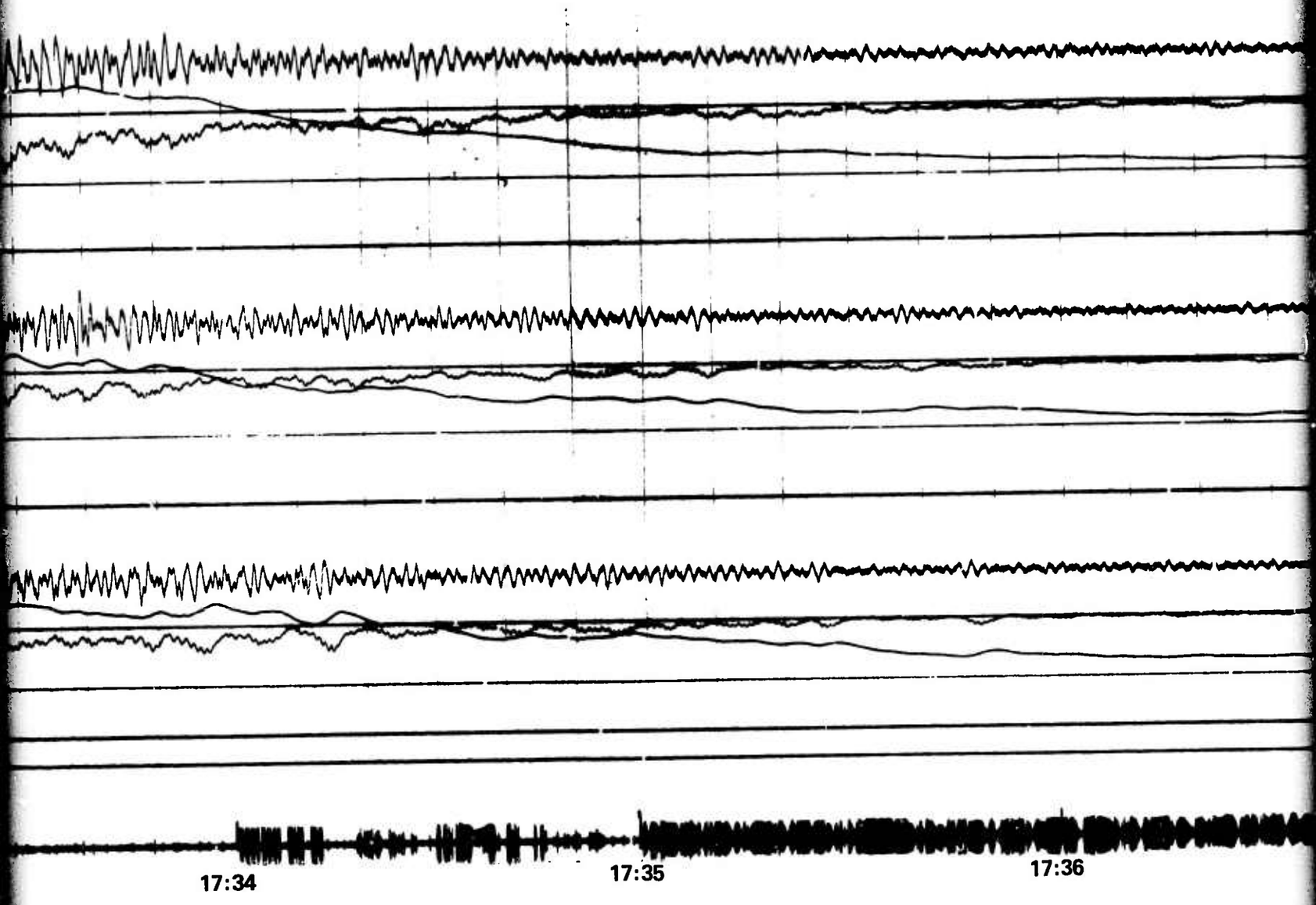
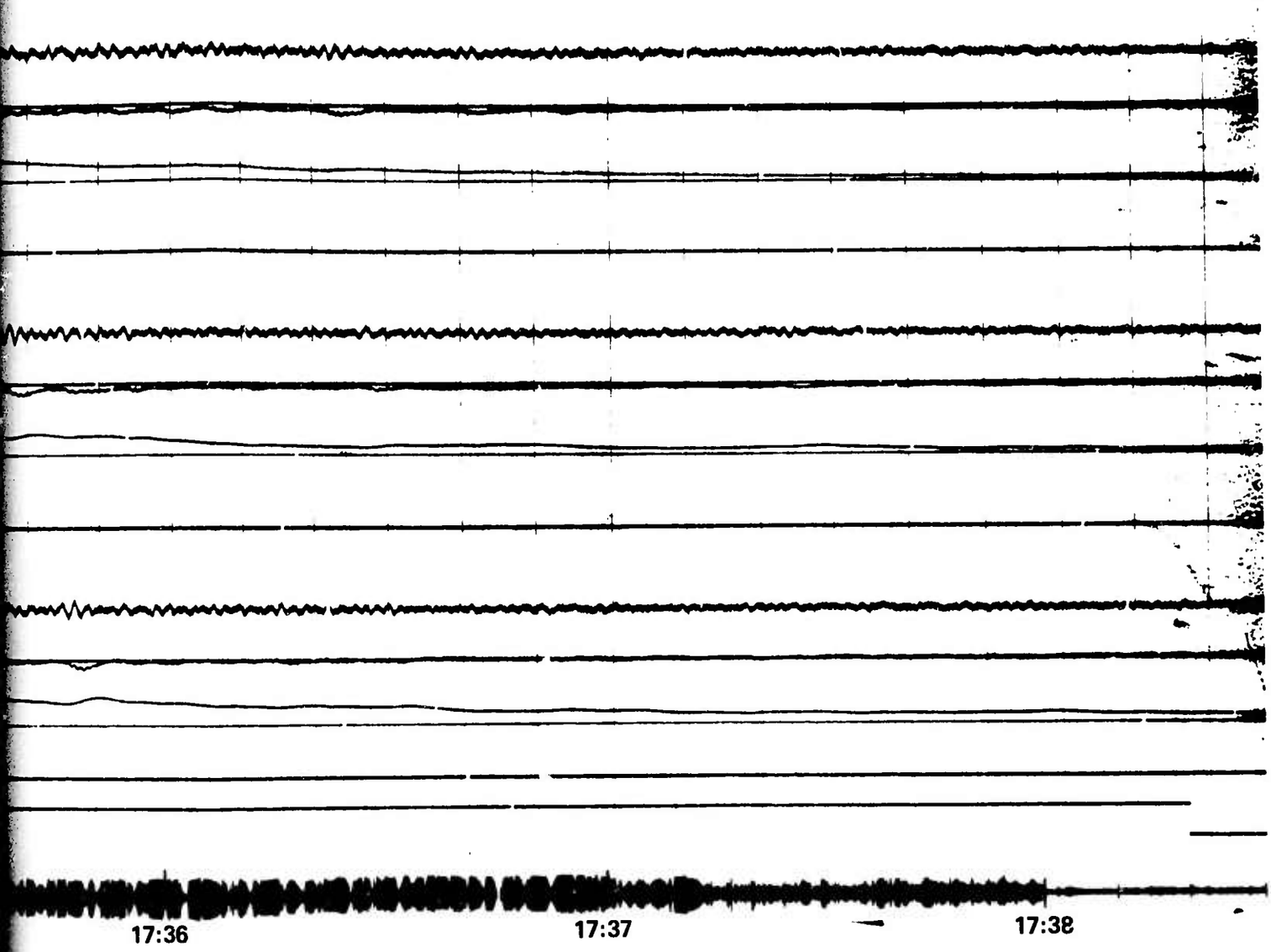



Figure D-4. "Merlin" recorded at TFO.

B




C



Preceding page blank

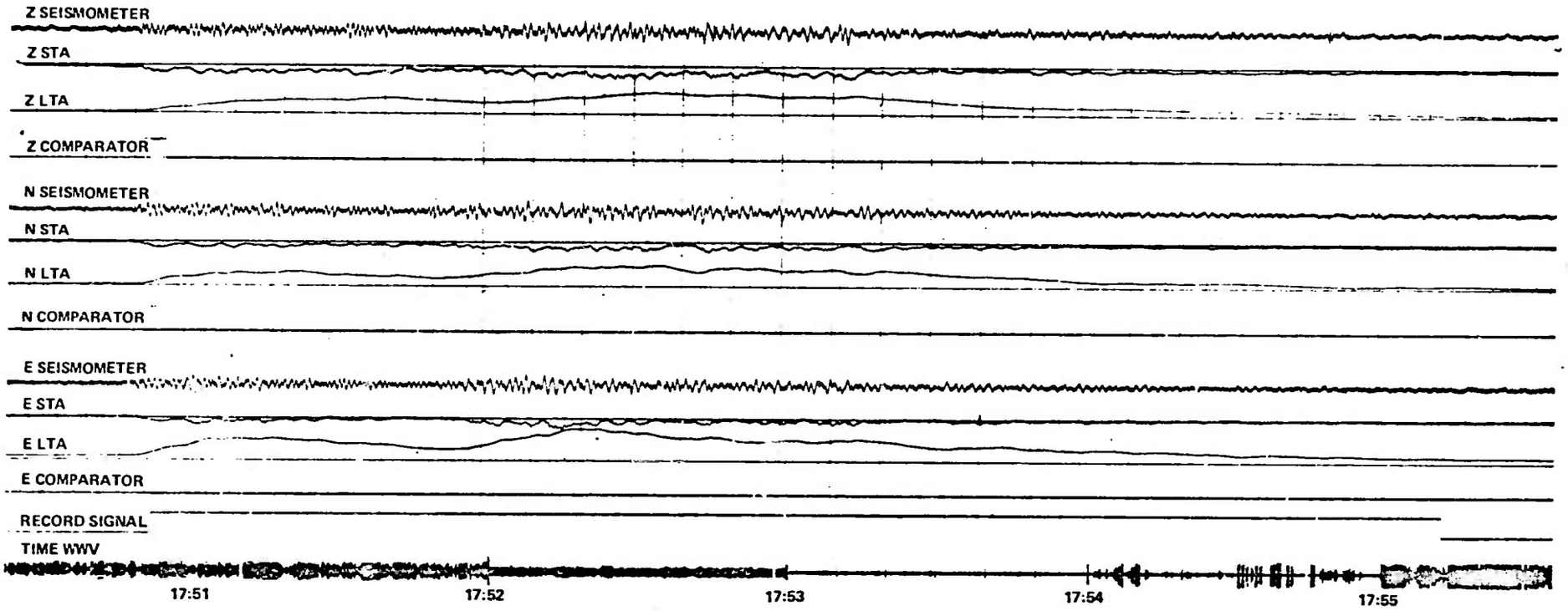



Figure D-5. Uncatalogued event recorded at TFO.



Preceding page blank

LIST OF REFERENCES


1. Van Trees, Harry L., Detection, Estimation, and Modulation Theory, Part I, John Wiley and Sons, Inc., New York, 1968, pp. 247 to 249.

2. Seismic Array Design Handbook, Federal Systems Division, IBM Corp., ARPA Order No. 800, August 1972, pp. 5-12 to 5-14.

3. Seismic Methods for Monitoring Underground Explosions, International Institute for Peace and Conflict Research (SIPRI), Sweden, 1968, p. 45.